6. Formulation Development and Evaluation of NLCs

6.1 Introduction

The aim of this study was to formulate and evaluate nanostructured lipid carriers (NLCs) for the topical application of Luliconazole and Tavaborole. NLCs are specialized colloidal delivery systems that combine a liquid lipid phase with a solid lipid matrix, often stabilized by surfactants (1-3). These carriers have been shown to improve the delivery of therapeutic agents through the skin and nails (4-10). The study used a Quality by Design (QbD) approach, incorporating statistical experimental designs, to explore how material attributes and process variables impact the formulation's key properties (11).

6.2 Materials and Instruments

Table 6.1 List of Materials

Chemical/Reagent	Manufacturer/Supplier
Luliconazole	Sun Pharmaceutical Industries Ltd., Vadodara
Tavaborole	Symed labs limited, Hyderabad
Methanol (A.R & HPLC grade)	Spectrochem Pvt. Ltd., Mumbai
Capmul MCM C8	Abitec Corporation, USA
Softemul AS	Mohini Organics, Mumbai
Softemul SE	Mohini Organics, Mumbai
Cremophore EL	Sigma Aldrich, India
Pluronic F 127	Sigma Aldrich, India
Distilled water	Prepared in house
Carbopol 974 P	Lubrizol, India
Propylene glycol	Astron Pharmaceutical Pvt. Ltd., India
Edetate disodium	Himedia, India
Triethanolamine	Loba Chemie Pvt. Ltd., India

Table 6.2 List of Equipments

Equipment/Instrument	Manufacturer/Supplier
Digital Analytical Balance	Shimadzu, Japan
RP-HPLC with UV detector (gradient)	Agilent, Germany
pH meter	Lab India Pvt. Ltd., Mumbai
Magnetic Stirrer	Remi equipment Pvt. Ltd., India
Vortex mixer	Spinix, Japan
Ultraturrax T25	IKA, Mumbai
Probe Sonicator	Labman Scientific Instruments Pvt. Ltd.
Centrifuge	Remi Instrument, India
Bath Sonicator	Remi equipment Pvt. Ltd., India
Particle Size Analyser (Nano-ZS)	Malvern Instrument, UK
Distillation assembly	Durga glassware, India
Brookfield Viscometer	Brookfield Engineering Laboratories, USA
Transmission electron microscope	JEOL, Japan
Ultrasonic Homogenizer	Sartorius Pvt Ltd. Germany

6.3 Methodology

6.3.1 Preparation of Luliconazole loaded NLCs (LZ NLCs) and Tavaborole loaded NLCs (TB NLCs):

The hot melt emulsification method was used to create LZ NLCs and TB NLCs, which were then, dispersed using ultrasonic technology (12). To create a lipid-drug mix, 90 mg of softemul AS for LZ NLCs and softemul AE for TB NLCs, 60 mg of capmul MCM C8, and 100 mg of a lipid-soluble surfactant i.e cremophore EL were combined in a beaker along with 3 ml of acetone, which acted as a co-solvent. In this mixture 1% Luliconazole was added for LZ NLCs and 5% Tavaborole was added for TB NLCs. Next, the mixture was continuously stirred as it evaporated at 60°C. In parallel, 100 mg of a water-soluble surfactant i.e. pluronic F 127 was dissolved in 9.65 gm of distilled water, which had also been heated to 60°C while being constantly stirred, to create an aqueous solution. For fifteen minutes, this aqueous solution was gradually added to the lipid mixture while being stirred at 1200 rpm on magnetic stirrer. After

that, the resulting emulsion was exposed to three minutes of probe sonication amplitude of 40%, with the procedure conducted in an ice bath to maintain low temperatures.

6.3.2 QbD approach for the formulation development

Identification of the formulation, process, and environmental aspects that may affect the end product's qualities is crucial before any formulation is created. These variables were thoroughly categorized using an Ishikawa diagram for the high-energy generation of LZ NLCs and TB NLCs. (see Figure 6.1).

6.3.2.1 Quality Target Product Profile (QTPP)

A number of features were established inside the QTPP in order to guarantee the intended level of product quality when creating a dependable, accurate, and repeatable manufacturing process for NLCs. Critical quality attributes (CQAs) that were determined were particle size and %EE based on a thorough examination of the literature and initial experimental runs (13).

6.3.2.2 Optimizing Formulation using Box-Behnken Design (BBD)

The intricate process of optimization usually entails changing one variable at a time and seeing how the changes affect the result. BBD is a three-level statistical design that combines two-level factorial designs and components of incomplete block designs. BBD operates within a spherical design space and is renowned for its exceptional predictive capabilities. It is a cubic design that differs from 3-factor, 3-level Full Factorial Design and Central Composite Design (CCD) due to its fewer required runs and its unique structure that includes midpoints of each edge and a central replicate point. When examining quadratic response surfaces, it works especially well when extreme predictions are not the focus (14, 15). These strategic advantages of the BBD in formulation optimization led to its selection.

Table 6.3 outlines the selected values for the BBD variables, encompassing both independent variables and dependent response parameters.

Table 6.3 Selected values of variables for BBD

Variables	Levels (-1, 0, 1)
Independent variables	
A: Lipid Concentration (%)	1,1.5,2
B: Smix Concentration (%)	1,2,3
C: Sonication time (min)	2,3,4

Dependent variables (Response parameters)
Particle size (Y1) (nm)
% EE (Y2) (%)

Important formulation elements were chosen in accordance with the findings from preliminary studies. A Box-Behnken Design (BBD) matrix was created using Stat-Ease Design-Expert Software 13.0, yielding 17 trial runs as shown in table no.6.3.2. All batches of LZ NLCs and TB NLCs were prepared in accordance with this design matrix while maintaining the same levels of other process variables. Critical quality characteristics (CQA) for the drug-loaded NLCs were determined to be particle size and % EE.

6.3.2.3 Preparation of checkpoint batches as per the overlay plot

After deriving and adding the data of the prepared batches based on the BBD, the data was analyzed by employing Design Expert 13.0 for optimized area. Checkpoint batches were prepared according to the three randomized points which were selected from the optimized area.

6.3.3 Characterization of NLCs containing Luliconazole and Tavaborole:

6.3.3.1 Particle Size, Polydispersity Index (PDI), and Zeta Potential:

A filtered sample of distilled water was used to dilute the NLC dispersion ten times. After that, the diluted sample was put into a cuvette for examination. Particle size, PDI, and zeta potential were measured using Dynamic Light Scattering (DLS) with a Nano-ZS Zetasizer from Malvern Instruments Ltd., UK (16).

6.3.3.2 %Entrapment Efficiency (%EE):

In order to determine the percentage of drug entrapment, the NLC dispersion was centrifuged for 30 minutes at 4 °C at 18,000 rpm. After that, the precipitated NLCs were dissolved in methanol in order to be subjected to an analytical procedure that had already been established. The supernatant was also checked for any unentrapped Tavaborole and Luliconazole in order to verify drug mass balance by using developed UV spectroscopic method for Luliconazole and HPLC method for Tavaborole (as mentioned in chapter 4). Using below equations, the mass of the drug within the centrifuged NLC pellet was utilized to determine the percentage of drug loading and entrapment (17, 18).

$$\%Entrapment\ efficiency\ (\%EE) = \left(\frac{amount\ of\ entrapped\ drug}{total\ drug\ added}\right) x\ 100$$

$$\%\ Drug\ loading\ = \frac{Weight\ of\ the\ drug\ in\ nanoparticles}{weight\ of\ the\ nanoparticles}\ x\ 100$$

6.3.3.3 Head Space Gas Chromatography (HS-GC) Testing for residual solvent:

Residual solvent present in the formulations were evaluated using gas chromatography (GC). To ascertain the acetone content, analysis was performed on the optimized batches of TB and LZ NLCs (19).

6.3.3.4 Differential scanning Calorimetry (DSC):

Differential Scanning Calorimetry (DSC) was used to examine the drug's thermal characteristics using a DSC-41 device (Shimadzu, Japan). The temperature range of 25°C to 300°C was applied to samples weighing 2-3 mg at a rate of 10°C/min while they were sealed inside an aluminium pan under pressure. To avoid oxidation, a nitrogen atmosphere was kept at a flow rate of 40 ml/min (20).

6.3.3.5 Transmission Electron Microscopy (TEM):

Using negative-staining electron microscopy, the morphology and nanostructure of the TB and LZ NLCs were investigated. Samples were positioned on copper/palladium grids covered with carbon for a minute, after which they were rinsed with deionized, sterile water and stained with 2% ammonium molybdate (pH 6.5). A JEOL JEM 2100 transmission electron microscope operating at 100 kV was used to make the observations (21).

6.3.3.6 Powder X-Ray Diffraction Studies:

Using a Rigaku-Miniflex powder X-ray diffractometer, the crystallinity of Luliconazole and its lyophilized NLCs (Lyophilization parameters: freezing stage -40 ºC, drying at 20 ºC, vaccum 120 mm Hg, time 48 hrs) was assessed. Cu Kα radiation was applied to the samples at 30 kV and 25 ºC for a 2θ range of 10–40º (22).

6.3.4 Preparation of gel of Luliconazole and Tavaborole loaded NLCs:

To improve viscosity and skin adhesion, a gel formulation of strengths 1% w/w and 5% w/w of Luliconazole and Tavaborole respectively, along with their corresponding optimised NLCs were formulated. Carbopol 974P was chosen as the gelling agent because to its exceptional ability to hydrate (23). Using magnetic stirrer at 1200 rpm, the carbopol 974P was mixed into the NLC

dispersions at a concentration of 1% w/w. Continuous mixing was used to integrate propylene glycol (4% w/w). Triethanolamine was used to set the pH range of 5.5 to 6.5.

6.3.5 Characterization of optimized Luliconazole and Tavaborole NLCs based gel

6.3.5.1 Viscosity of gel

Using a T-bar No. 96 spindle, viscosity measurements were performed with a Brookfield DV-I prime viscometer (24).

6.3.5.2 pH of gel

The pH of the free Luliconazole gel, free Tavaborole gel, LZ NLCs based gel and TB NLCs based gel were determined using a pH meter from Lab India Pvt. Ltd., Mumbai (25).

6.3.5.3 Spreadability of gel

The spreadability of free Luliconazole gel, LZ NLCs containing gel, free Tavaborole gel, TB NLCs containing gel was assessed by a following method. A fixed quantity (150 mg) of each gel was placed within a marked circle on a glass plate, covered with another glass plate, and subjected to a weight of 10 g for five minutes; the time that needed for upper plate to completely separate from the lower plate is measured. Spreadability was determined by the below equation (26).

$$Spreadability = \frac{M\ x\ L}{T}$$

Where, M – weight in gm placed on upper plate, L – length of plate, T – time taken to separate

6.3.5.4 Assay

Luliconazole and Tavaborole concentrations in the different gel formulations were measured by dissolving 100 mg of the sample in methanol and utilizing a gradient HPLC method described in sections 3.3 and 3.4 of chapter 3 to analyze it (27).

6.3.5.5 Gel Strength

A 10 kg load cell equipped with a Brookfield Engineering CT3 texture analyzer was utilised to assess the mechanical characteristics of developed LZ NLCs based gel and TB NLCs based gel. To evaluate the gel strength, the sample was put into a cone fixture, leveled, and tested using a TA3/100 probe at pre-test and test speeds of 1 mm/s and 0.5 mm/s, respectively (28).

6.4 Results and Discussion

6.4.1 Preparation of Luliconazole and Tavaborole loaded NLCs

6.4.1.1 Defining QTPP:

Table 6.4: QTPP and CQA elements with justification for LZ NLCs

QTPP elements		Target	Justification
Route of administration		Topical	To effective permeation of drug and deposition of drug in skin for better topical delivery of product and reduce systemic side effect.
Dosage form		NLCs	Better skin permeability, controlled release of drug
Formulation quality attributes	Particle size*	Optimum	For better permeation as well as skin deposition. To prevent drug entry in blood circulation.
	Polydispersity index (PDI)	Minimum (<0.3)	To ensure formation of monodisperse formulation
	Shape		To ensure formation of NLCs
	Zeta potential	>±30 mV	For the enhancement of stability of the dispersion
	% EE *	Maximize	For the reduction of cost, drug wastage to be reduced
	In-vitro drug release	For 24 hrs	To ensure controlled release of drug.
Ex-vivo permeability		Maximize	To ensure effective permeation of drug.
Stability		Not less than 3 month	For ensuring stability of developed formulation during its complete shelf life
Safety		Non-toxic and non-irritant to skin	To ensure prevent skin irritation and cell toxicity

Pharmacodynamic	Similar or better than marketed product	For the illustration of therapeutic efficacy

* Critical Quality Attributes (CQAs)

Three factors were shown to be affect the development of Tavaborole and Luliconazole loaded NLCs using the high energy method: Environment, Process, and Formulation. The variables related to the formulation of Tavaborole and Luliconazole loaded NLCs were illustrated using the Ishikawa diagram (Figure 6.1).

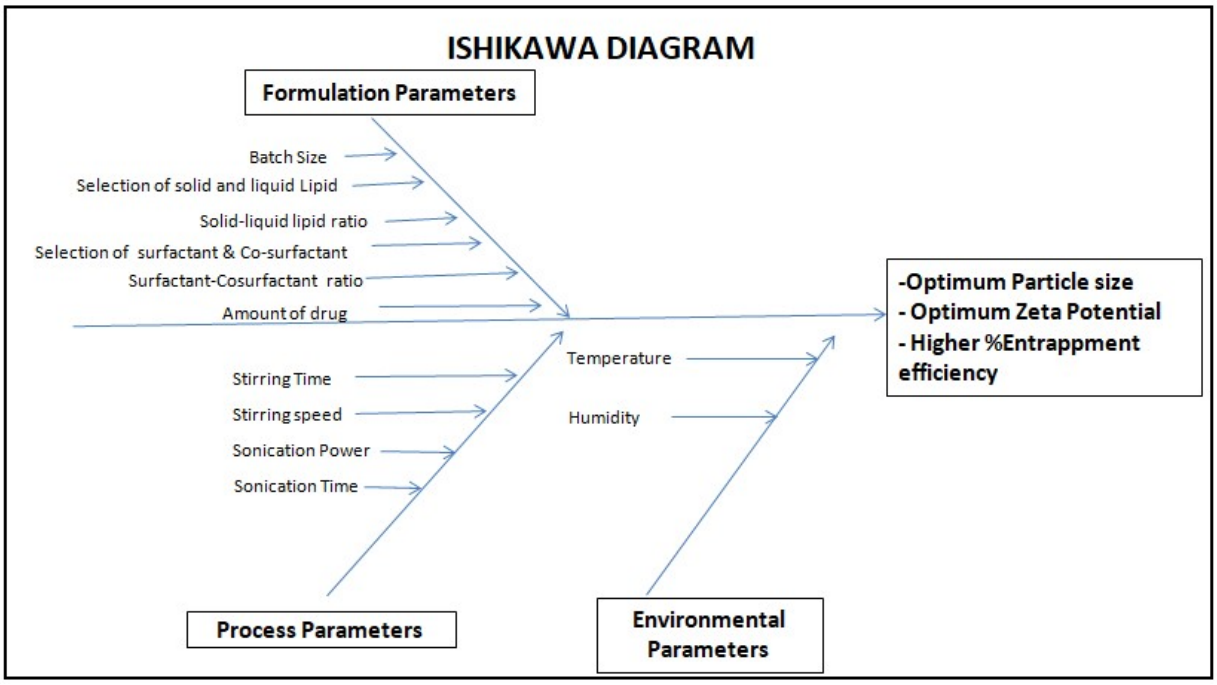

Figure 6.1 Ishikawa diagram showing probable variables that may influence CQA

6.4.2.2 Formulation optimization by Box-Behnken Design for Luliconazole loaded NLCs

Three crucial process parameters (CPP) were identified based on the preliminary analysis, and Box-Behnken Design was used to thoroughly analyse their link with critical quality attributes. Using the Design-Expert software, a randomised matrix including 17 runs was created, and it is shown in the table 6.5.

Table 6.5: Randomized BBD design matrix generated Design-Expert software

Run	Independent Variables			Dependent Variables (CQA)	
	A:Lipid concentration (%)	B:Smix Concentration (%)	C:Sonication time (Min)	Particle size (nm)	% EE
1	2	2	2	272.33±0.49	70.32±0.03
2	2	3	3	218.57±0.34	69.98±0.61
3	1.5	3	4	192.00±0.07	74.49±0.09
4	1	2	4	198.09±0.72	58.76±1.07
5	1.5	2	3	237.08±0.59	79.17±1.33
6	1.5	2	3	241.09±1.37	80.21±0.69
7	1	1	3	230.57±0.24	55.61±1.04
8	1.5	2	3	239.00±0.05	79.94±0.98
9	1.5	2	3	242.44±0.87	80.47±1.27
10	1.5	2	3	240.00±0.03	80.36±0.34
11	1	3	3	248.33±0.77	60.09±1.77
12	1.5	1	2	269.13±0.61	71.52±0.95
13	1.5	1	4	186.27±0.34	70.65±0.07
14	1.5	3	2	275.05±1.28	77.82±0.46
15	2	1	3	227.64±0.08	65.43±0.67
16	1	2	2	279.33±1.67	58.97±1.43
17	2	2	4	184.00±0.31	69.83±1.65

6.4.2.3 Effect analysis of critical variables on responses

6.4.2.3.1 Influence of investigated parameters on Particle size

A) Statistical Analysis for Particle size

The statistical analysis of the design mentioned above is as follows:

Table 6.6 Statistical analysis of design for Particle size

Source	Sequential p-value	Lack of Fit p-value	Adjusted R^2	Predicted R^2	
Linear	< 0.0001	0.0105	0.9595	0.9432	
2FI	0.1529	0.0140	0.9682	0.9480	
Quadratic	**0.0013**	**0.2827**	**0.9946**	**0.9768**	**Suggested**
Cubic	0.2827		0.9960		**Aliased**

As shown in Table 6.6, the best model to fit the experimental results of Particle size in NLCs is the quadratic model and was chosen for further evaluation.

B) ANOVA Analysis for Particle size

The ANOVA for Particle size is given in below Table.

Table 6.7 ANOVA for Response Surface Quadratic Model for Particle size

Source	Sum of Squares	Df	Mean Square	F- value	p-value	
Model	14903.89	9	1655.99	330.73	< 0.0001	significant
A-Lipid Concentration	364.50	1	364.50	72.80	< 0.0001	
B-Smix Concentration	55.12	1	55.12	11.01	0.0128	
C-Sonication time	14028.13	1	14028.13	2801.62	< 0.0001	
AB	182.25	1	182.25	36.40	0.0005	
AC	12.25	1	12.25	2.45	0.1618	
BC	0.0000	1	0.0000	0.0000	1.0000	

A^2	41.78	1	41.78	8.34	0.0234	
B^2	146.57	1	146.57	29.27	0.0010	
C^2	48.67	1	48.67	9.72	0.0169	
Residual	35.05	7	5.01			
Lack of Fit	20.25	3	6.75	1.82	0.2827	not significant
Pure Error	14.80	4	3.70			
Cor Total	14938.94	16				

The model is significant, according to the model's F-value of 330.73. This high F-value has a 0.01% probability of being caused by noise. Model terms are considered significant when P-values are less than 0.0500. A, B, C, AB, A^2, B^2, and C^2 are important model terms in this instance. The model terms are not important if the value is greater than 0.1000.

In comparison to the pure mistake, the Lack of Fit appears to be insignificant, as indicated by the F-value of 1.82 for the lack of fit. A big F-value for lack of fit could be the result of noise with a probability of 28.27%. Fit is desirable; a non-significant deficiency in fit is desirable.

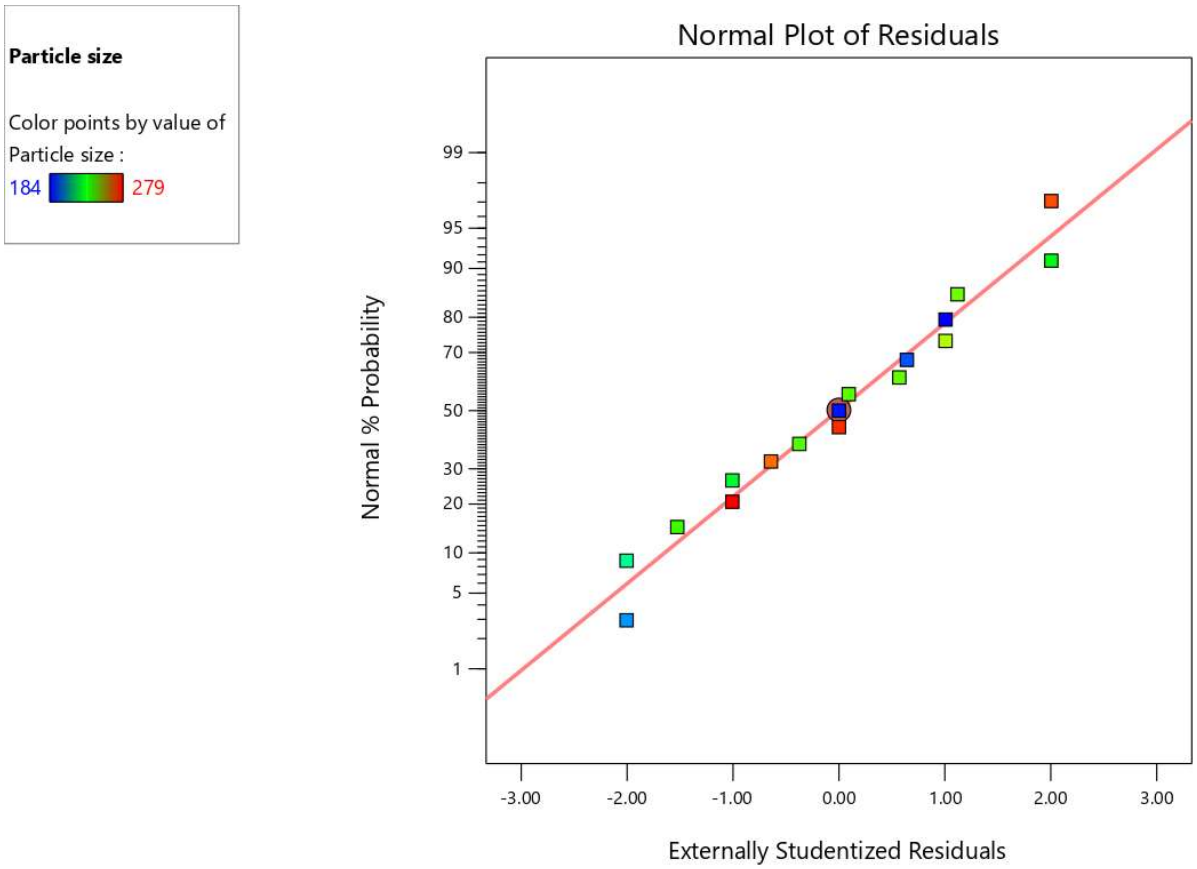

Figure 6.2 Actual v/s Predicted plot for % Particle size

Table 6.8 ANOVA study results for Particle size

Parameters Results of Response	Parameters Results of Response
Std Deviation	2.24
Mean	233.94
C.V.%	0.9565
R-Squared	0.9977
Adjusted R-Squared	0.9946
Predicted R-Squared	0.9768
Adeq. Precision	56.6655

There is less than 0.2 differences between the Adjusted R^2 of 0.9946 and the Predicted R^2 of 0.9768, indicating a satisfactory agreement. Adeq Precision calculates the ratio of signal to noise.

Ideally, the ratio should be higher than 4. Signal strength, 56.666, is sufficient. The design area can be navigated with the help of this model.

C) Mathematical Model for Particle size

In addition to the ANOVA value, contour plots and three-dimensional plots were used to investigate the impact of different factors on particle size. Table 6.8 shows that the ultimate reaction, or particle size, confirms the influence of different components when the combination of different degrees of factors changes. Examining the various contributing factors in detail helps us to better grasp the magnitude of the effect. Positive and negative effects are discussed in the equation.

The final equation in terms of coded factors:

Particle size: $+239.80+6.75*A+2.62*B-41.88*C-6.75*AB-1.75*AC+0.0180*BC-3.15*A^2-5.90*B^2-3.40*C^2$

Table 6.9 The Final equation in terms of actual factors:

Particle Size	=
+239.80	
+6.75	Lipid Concentration
+2.62	S_{mix} Concentration
-41.88	Sonication time
-6.75	Lipid Concentration * S_{mix} Concentration
-1.75	Lipid Concentration * Sonication time
+0.0180	S_{mix} Concentration * Sonication time
-3.15	Lipid Concentration^2
-5.90	S_{mix} Concentration^2
-3.40	Sonication time^2

The presence of a positive sign preceding a factor signifies an increase in response with the factor and vice versa. Furthermore, it can be seen from the preceding equation that each element has some effect on particle size. Two of the three independent variables that were selected have positive effects on particle size and one of the three independent variables that were selected

have negative effects on particle size as shown by the coefficient values of the individual factors. The highest co-efficient value before factor C indicates that sonication time has the greatest impact on particle size, which is followed by lipid concentration and S_{mix} Concentration. As an example, particle size increases when lipid concentration and S_{mix} increases. An increase in sonication time was shown to cause a decrease in particle size. It may be because of the disruption of the particles caused by an increase time of sonication (29).

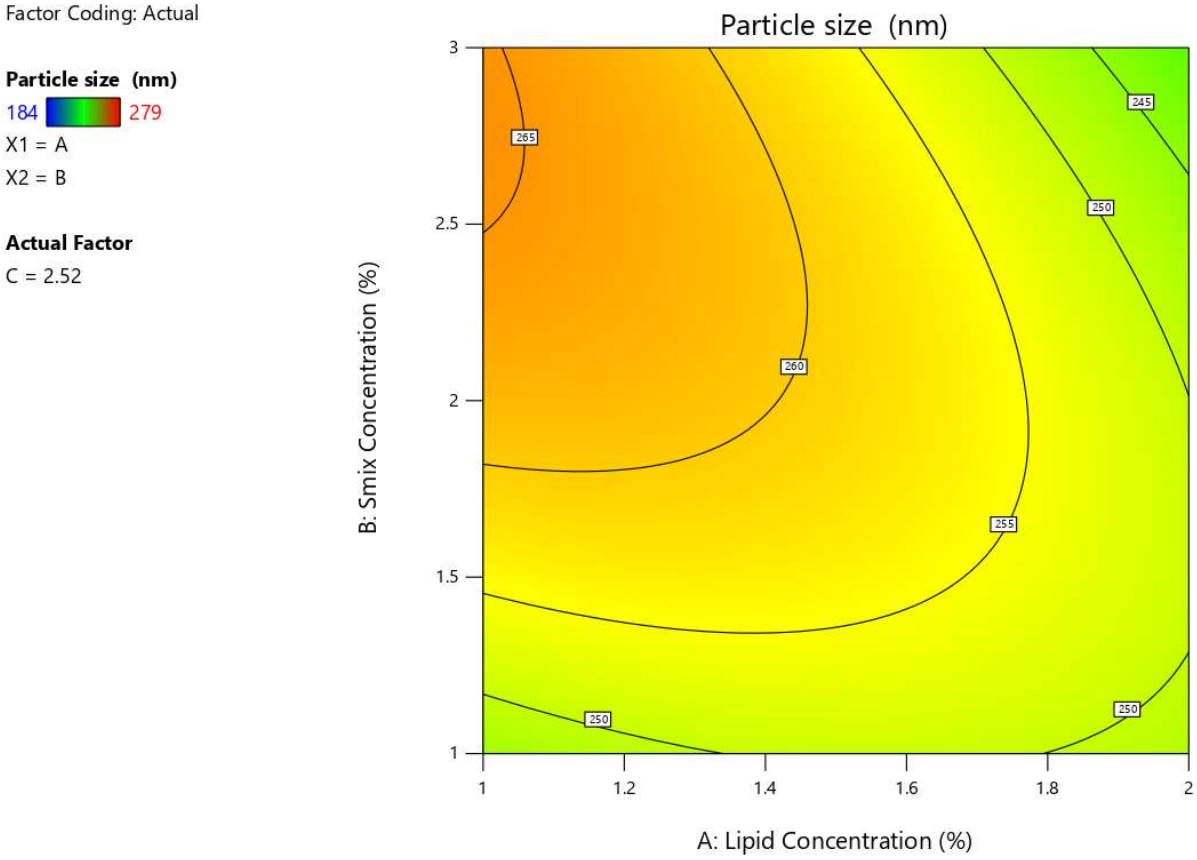

Figure 6.3 Contour plot (2D) showing the combined effect of Smix concentration and lipid concentration on Particle size

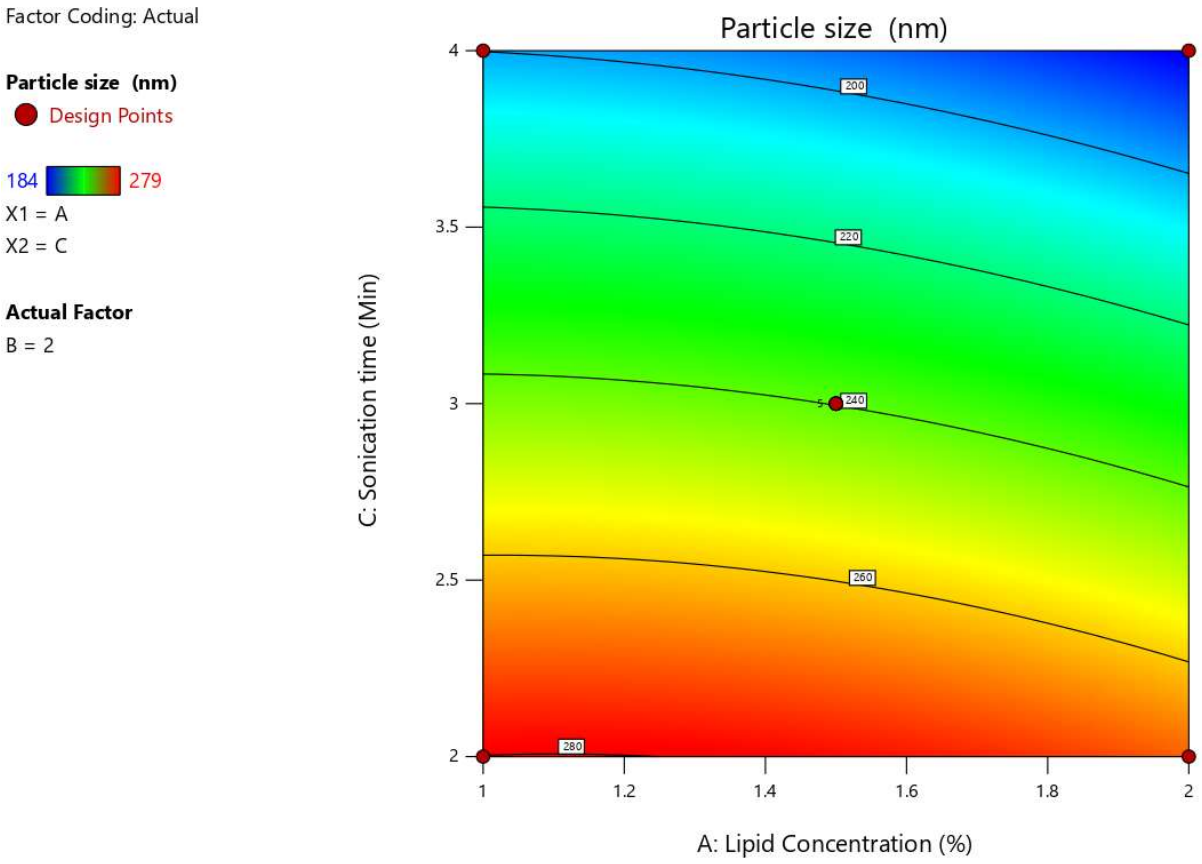

Figure 6.4 Contour plot (2D) showing the combined effect of lipid concentration and sonication time on Particle size

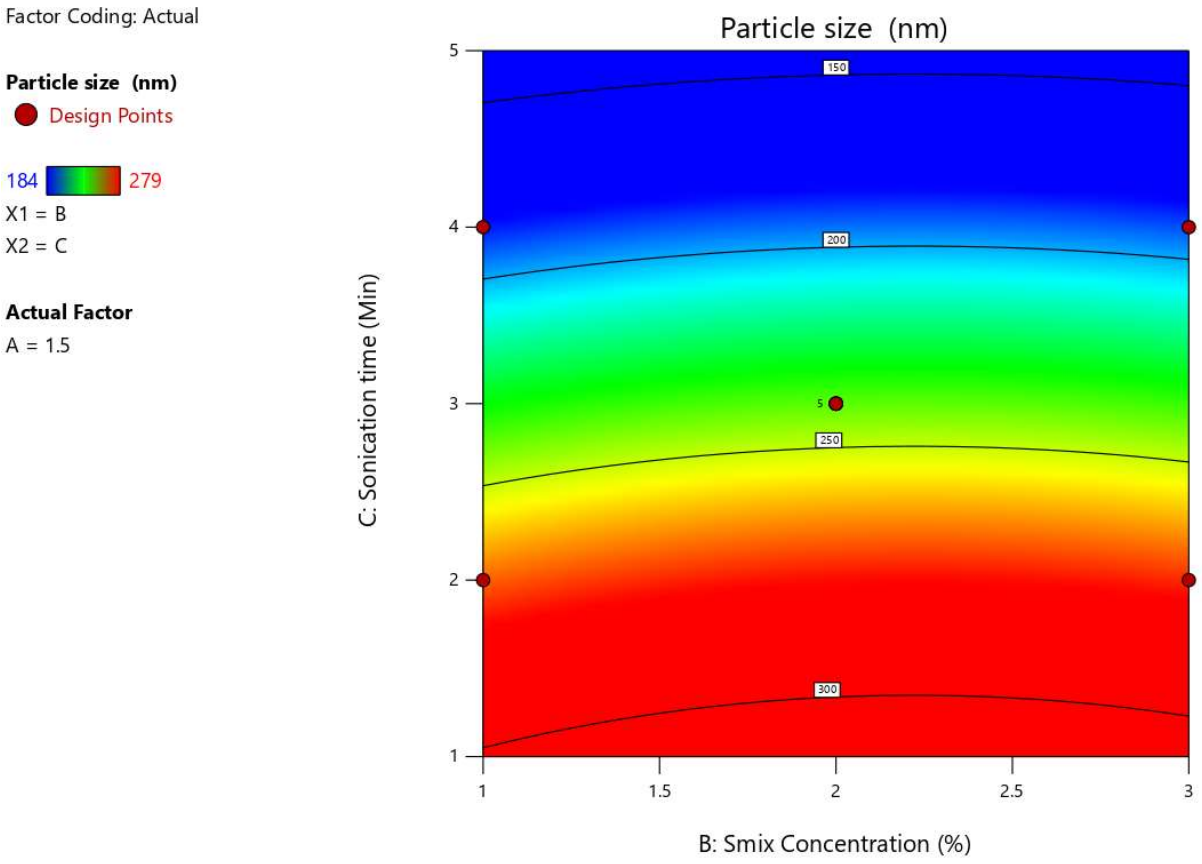

Figure 6.5 Contour plot (2D) showing the combined effect of sonication time and Smix concentration on Particle size

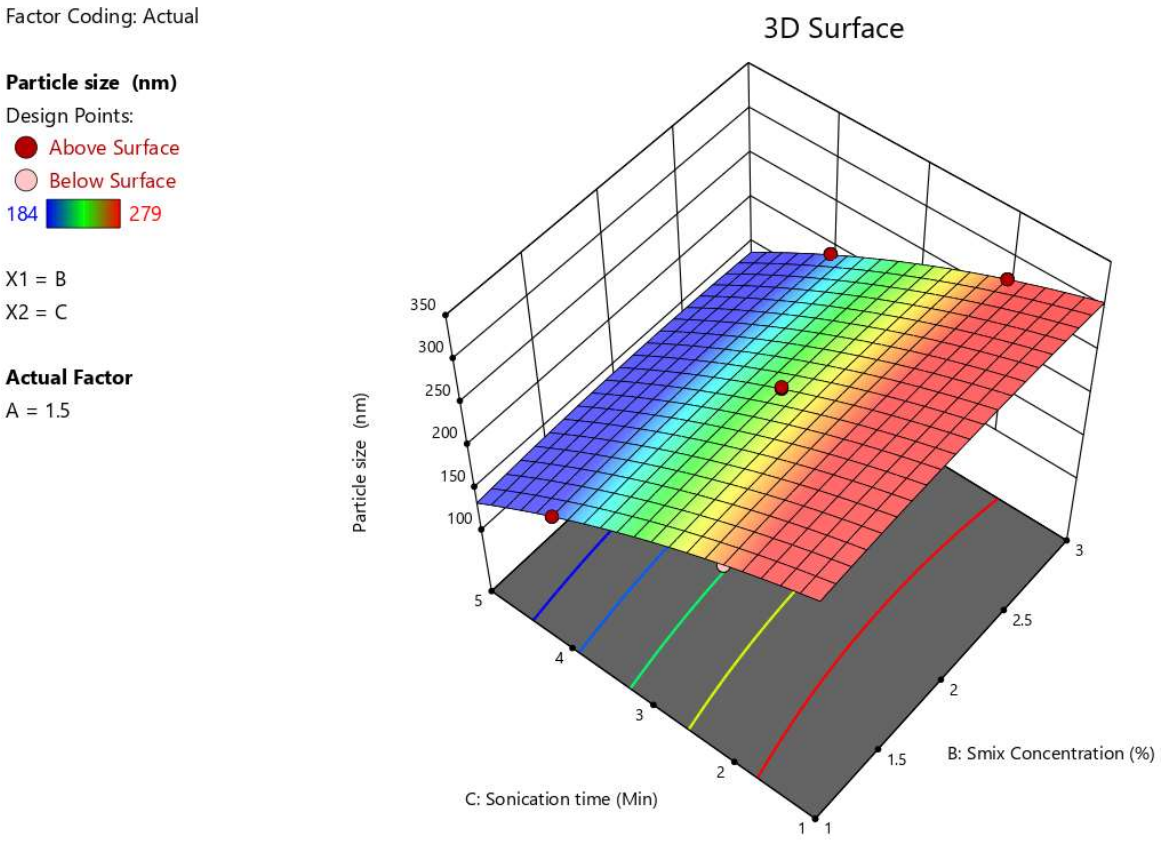

Figure 6.6 Response surface (3D) showing the combined effect of Smix concentration and Sonication time on Particle size

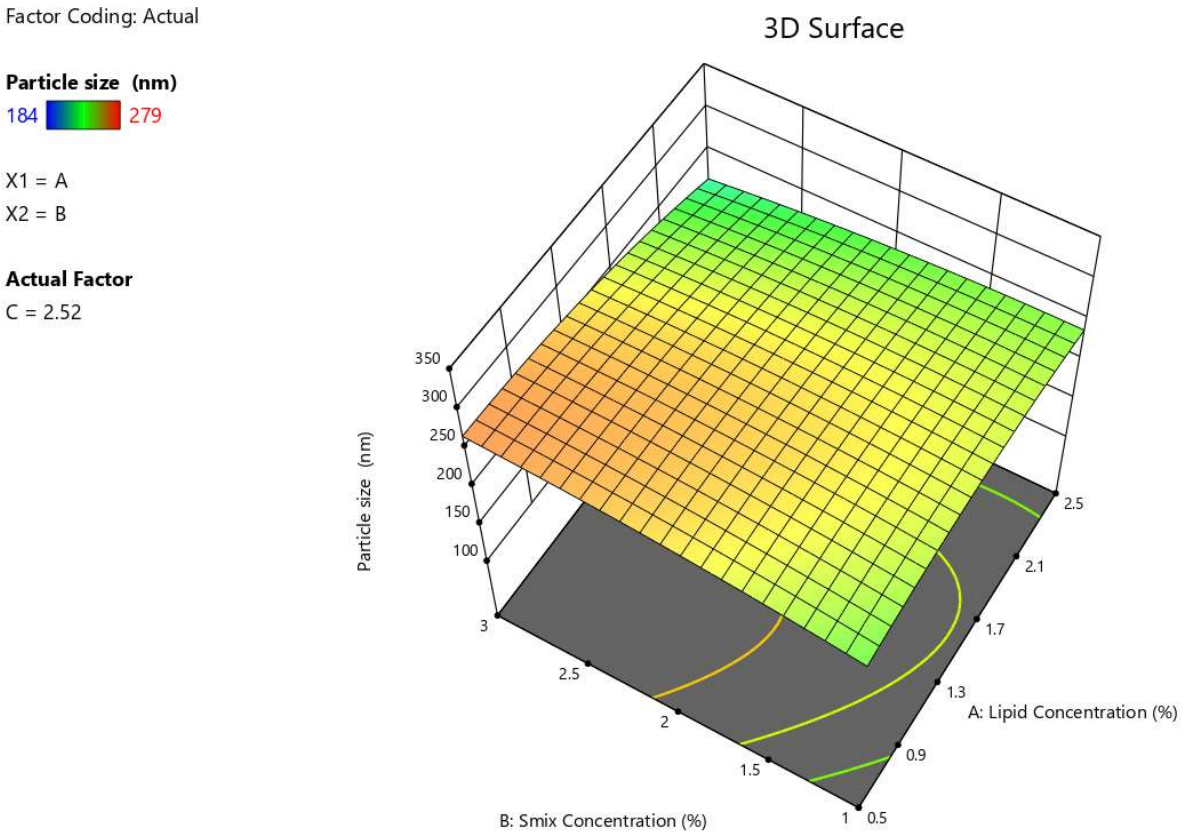

Figure 6.7 3D surface graph showing the combined effect of lipid concentration and Smix concentration on Particle size

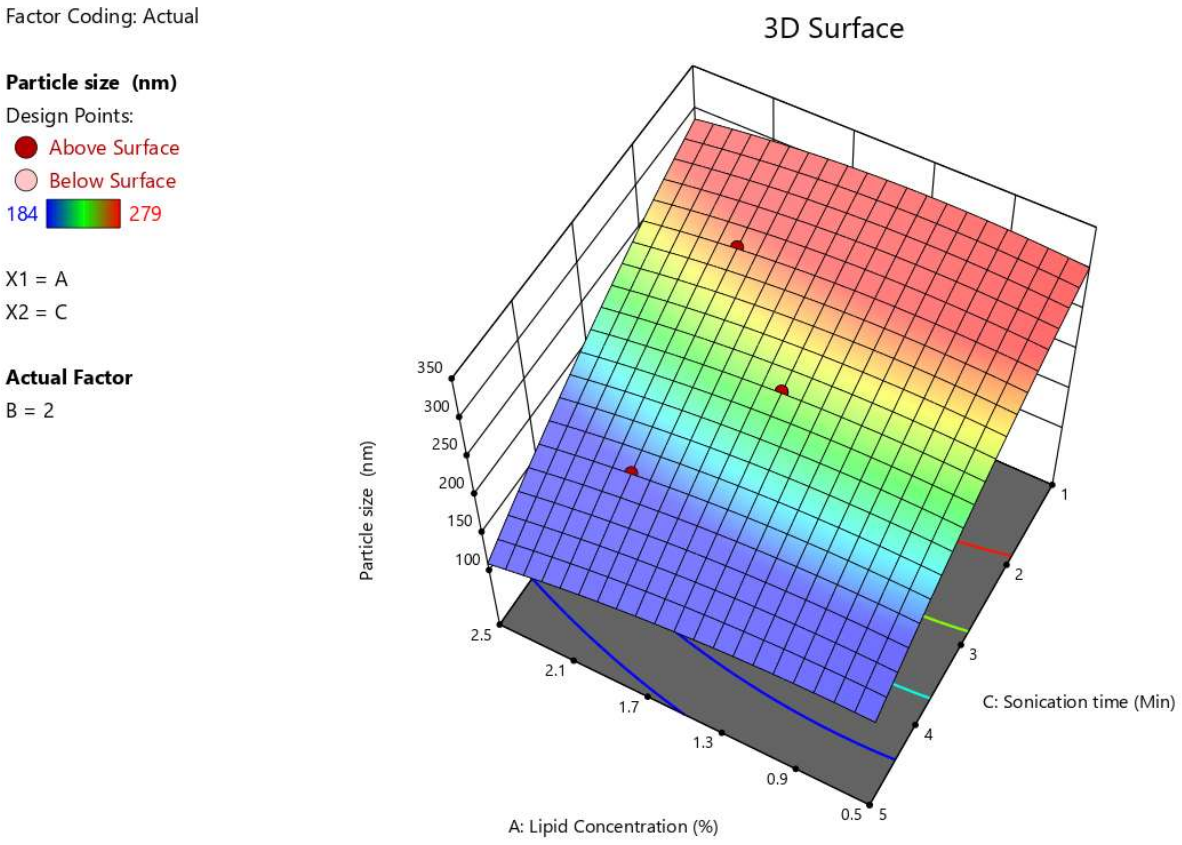

Figure 6.8 3D surface graph showing the combined effect of lipid concentration and sonication time on Particle size

The effects of independent factors on the particle size are shown in figure 6.4 to figure 6.8. The largest particle size is shown by the red area, and the lowest particle size is represented by the blue zone. It can be depicted that particle size increases when lipid concentration and S_{mix} increases and particle size decreases as sonication time increases (30). These graphs show the relationship between the CQA and the corresponding independent factor while maintaining constant levels of the other independent variables.

6.4.2.3.2 Influence of investigated parameters on % EE

A) Statistical Analysis for Particle size

The statistical analysis of the design mentioned above is as follows:

Table 6.10 Statistical analysis of design for % EE

Source	Sequential p-value	Lack of Fit p-value	Adjusted R^2	Predicted R^2	
Linear	0.3065	< 0.0001	0.0587	-0.2434	
2FI	0.9993	< 0.0001	-0.2216	-1.4363	
Quadratic	**< 0.0001**	**0.1449**	**0.9927**	**0.9624**	**Suggested**
Cubic	0.1449		0.9962		**Aliased**

As shown in table 6.9, the best model to fit the experimental results of % EE in NLCs is the quadratic model and was chosen for further evaluation.

B**) ANOVA Analysis for % EE**

The ANOVA for Particle size is given in below table.

Table 6.11 ANOVA for Response Surface Quadratic Model for % EE

Source	Sum of Squares	Df	Mean Square	F- value	p-value	
Model	1147.83	9	127.54	242.21	< 0.0001	Significant
A-Lipid Concentration	221.87	1	221.87	421.36	< 0.0001	
B-Smix Concentration	45.94	1	45.94	87.24	< 0.0001	
C-Sonication time	3.00	1	3.00	5.70	0.0484	
AB	0.0012	1	0.0012	0.0023	0.9629	
AC	0.0196	1	0.0196	0.0372	0.8525	
BC	1.51	1	1.51	2.87	0.1339	
A^2	733.78	1	733.78	1393.55	< 0.0001	
B^2	69.11	1	69.11	131.24	< 0.0001	

C^2	23.43	1	23.43	44.49	0.0003	
Residual	3.69	7	0.5266			
Lack of Fit	2.60	3	0.8678	3.21	0.1449	not significant
Pure Error	1.08	4	0.2706			
Cor Total	1151.52	16				

A model's significance is indicated by its F-value of 242.21. Significant model terms are indicated by P-values less than 0.0500. This instance involves important model terms A, B, C, A^2, B^2, and C^2. The Lack of Fit is not significant relative to the pure error, as indicated by the 3.21 Lack of Fit F-value. An F-value for Lack of Fit this large has a 14.49% probability of being caused by noise. Fit is desirable; a non-significant deficiency in fit is desirable.

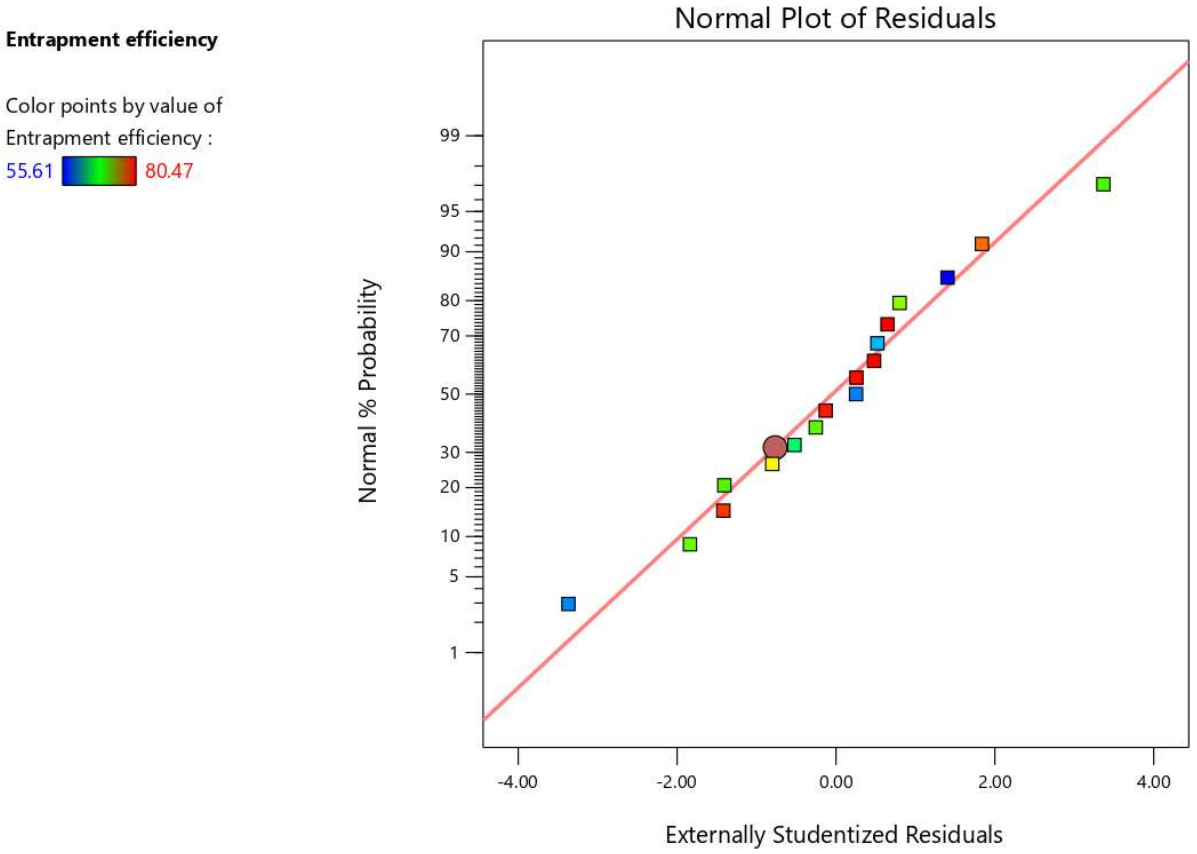

Figure 6.9 Actual v/s Predicted plot for % EE

Table 6.12 ANOVA study results for % EE

Parameters Results of Response	Parameters Results of Response
Std Deviation	0.7256
Mean	70.80
C.V.%	1.02
R-Squared	0.9968
Adjusted R-Squared	0.9927
Predicted R-Squared	0.9624
Adeq. Precision	44.7362

There is less than 0.2 discrepancies between the Adjusted R^2 of 0.9927 and the Predicted R^2 of 0.9624, indicating a reasonable agreement. Adeq Precision calculates the ratio of signal to noise. Ideally, the ratio should be higher than 4. A sufficient signal is shown by ratio of 44.736. The design area can be navigated with the help of this model.

C) Mathematical Model for % EE:

Contour plots and the 3D plot were used in conjunction with the ANOVA value to investigate the impact of different factors on the percentage of % EE. Table 6.11 shows that the final response, or % EE, confirms the impact of different factors when the combination of different amounts of factors changes. Examining the various contributing factors in detail helps us to better grasp the magnitude of the effect. Positive and negative effects are discussed in the equation.

The final equation in terms of coded factors:

% EE: $+80.03+5.27*A+2.40*B-0.6125*C+0.0175*AB-0.0700*AC-0.6150*BC-13.20*A^2-4.05*B^2-2.36*C^2$

Table 6.13 The Final equation in terms of actual factors

% EE	=
+80.03	
+5.27	Lipid Concentration
+2.40	S_{mix} Concentration
-0.6125	Sonication time

+0.0175	Lipid Concentration * S_{mix} Concentration
-0.0700	Lipid Concentration * Sonication time
-0.6150	S_{mix} Concentration * Sonication time
-13.20	Lipid Concentration^2
-4.05	S_{mix} Concentration^2
-2.36	Sonication time^2

The presence of a positive sign preceding a factor signifies an increase in response with the factor and vice versa. Furthermore, it can be seen from the preceding equation that each element has some effect on %EE. Two of the three independent variables that were selected have positive effects on %EE and one of the three independent variables that were selected have negative effects on %EE as shown by the coefficient values of the individual factors. As an example, % EE increases when lipid concentration and S_{mix} concentration increases. API partitioned into the lipidic phase, resulting in an increase in % EE with an increase in lipid concentration. An increase in sonication time was shown to cause a decrease in % EE (29).

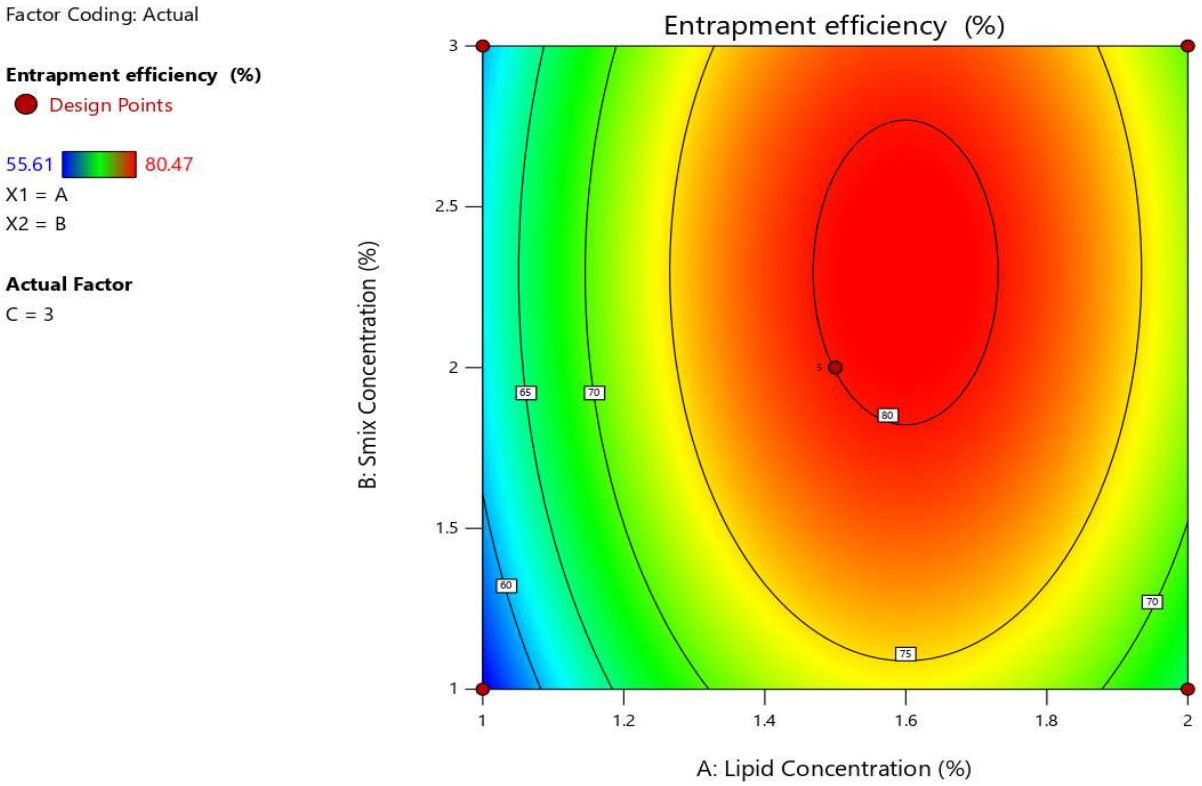

Figure 6.10 Contour plot (2D) showing the combined effect of Lipid concentration and Smix Concentration on % EE

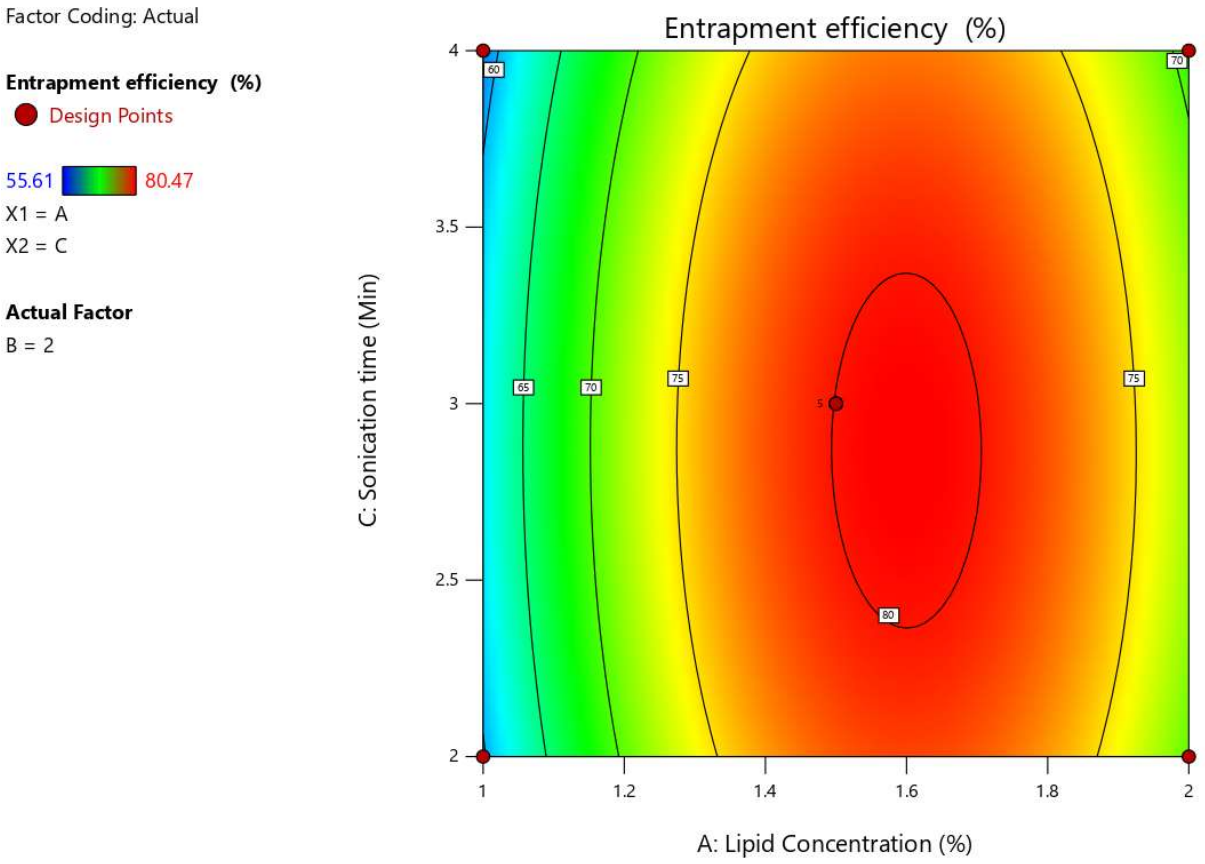

Figure 6.11 Contour plot (2D) showing the combined effect of Lipid concentration and Sonication time on % EE

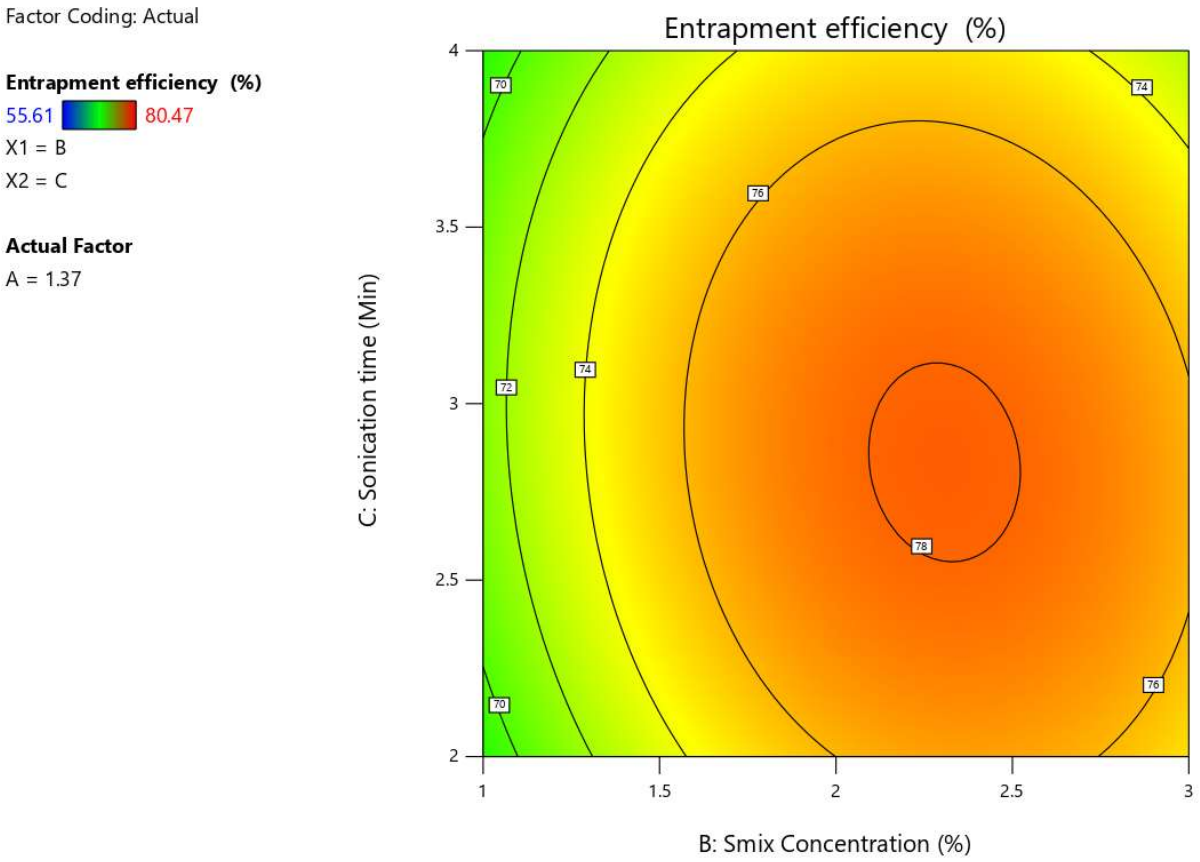

Figure 6.12 Contour plot (2D) showing the combined effect of Smix concentration and Sonication time on % EE

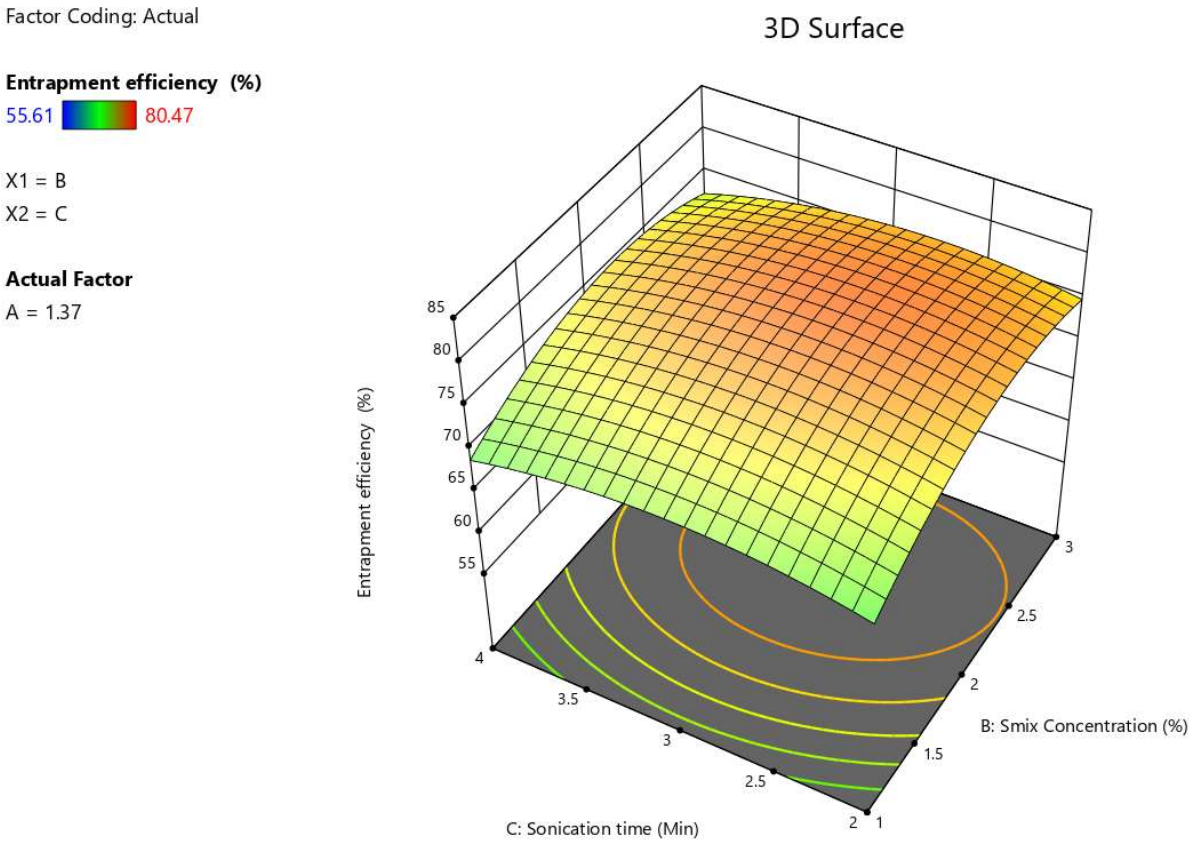

Figure 6.13 Response surface (3D) showing the combined effect of sonication time and Smix concentration on % EE

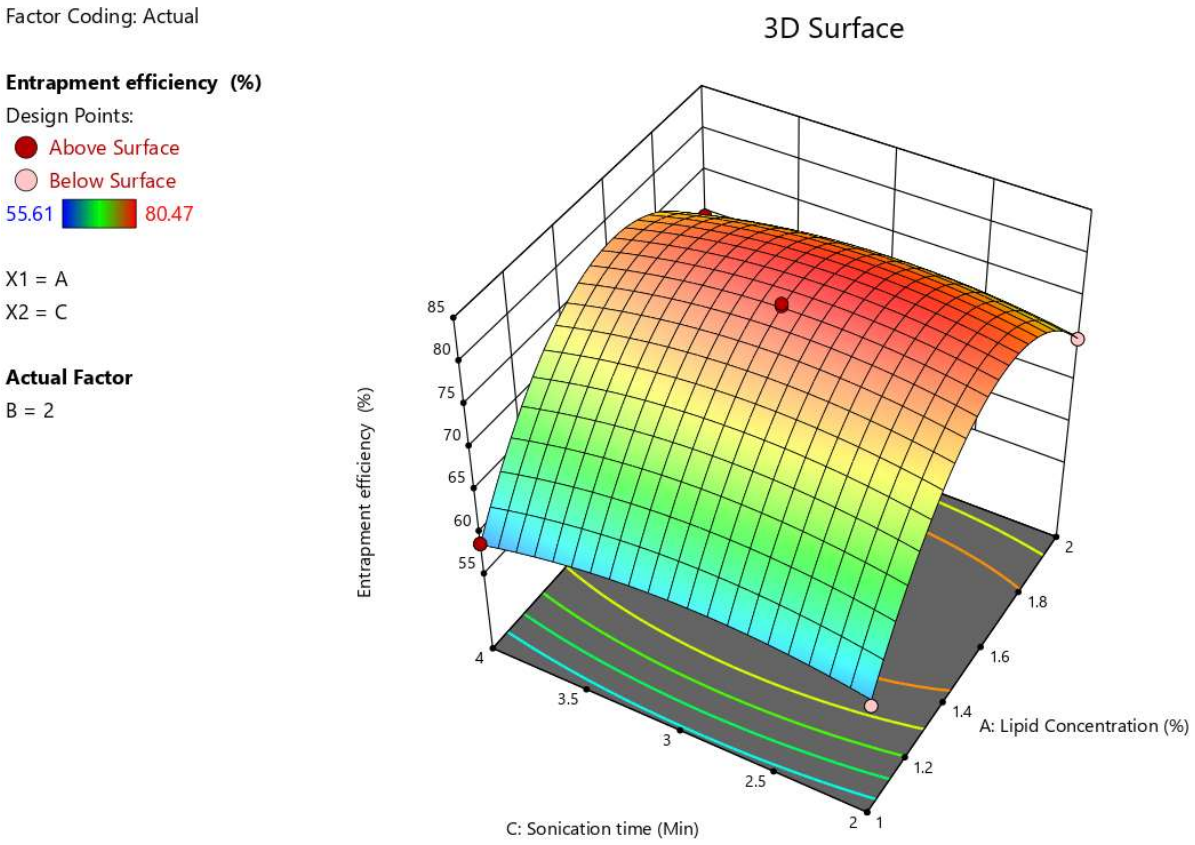

Figure 6.14 Response surface (3D) showing the combined effect of lipid concentration and Sonication time on % EE

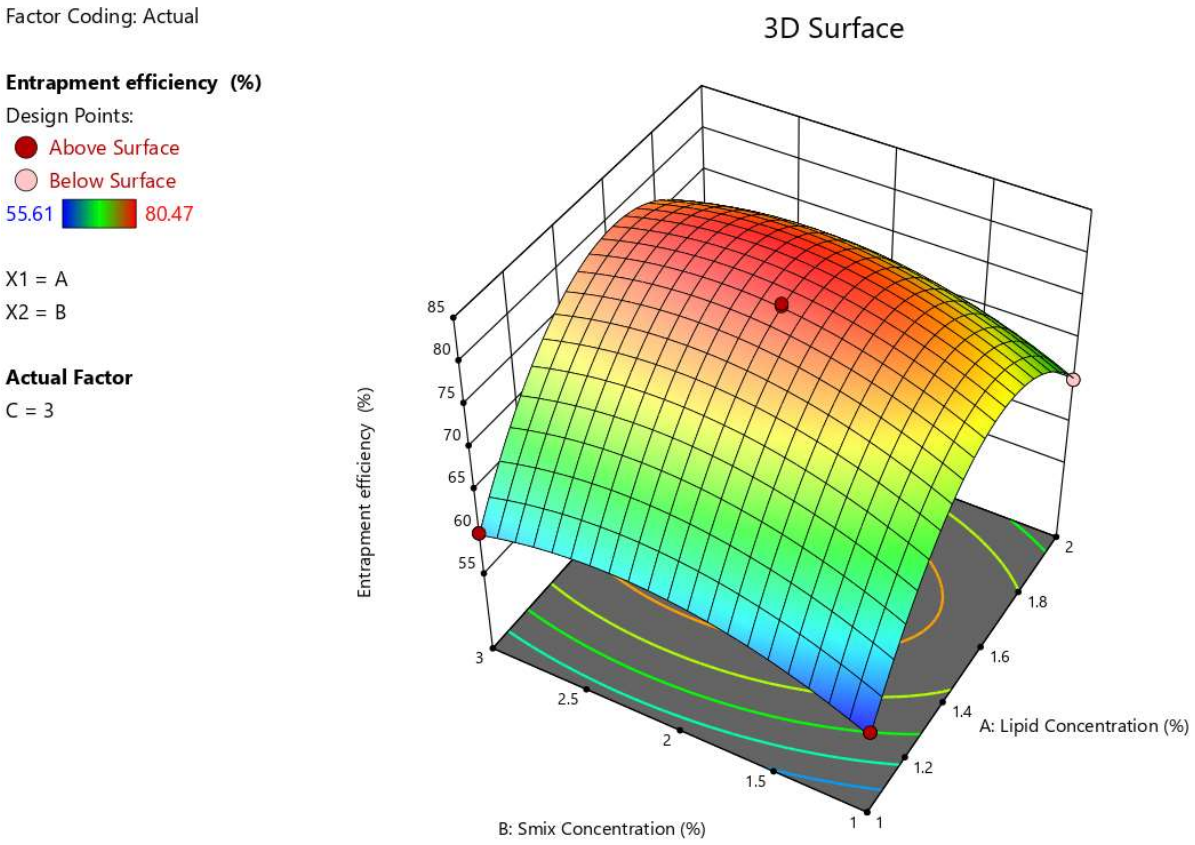

Figure 6.15 Response surface (3D) showing the combined effect of Smix concentration and Lipid concentration on % EE

The effects of independent factors on the % EE are shown in figure 6.10 to figure 6.15. The highest % EE is shown by the red area, and the lowest % EE is represented by the blue zone. It can be depicted that % EE increases when lipid concentration and S_{mix} concentration increases. An increase in sonication time was shown to cause a decrease in % EE (30). These graphs show the relationship between the CQA and the corresponding independent factor while maintaining constant levels of the other independent variables.

6.4.2.4 Preparation of checkpoint batches as per the overlay plot

Overlay contour plots for all two CQAs (%EE and particle size) were generated (Fig. 6.16) for obtaining the design space (yellow area in graph).

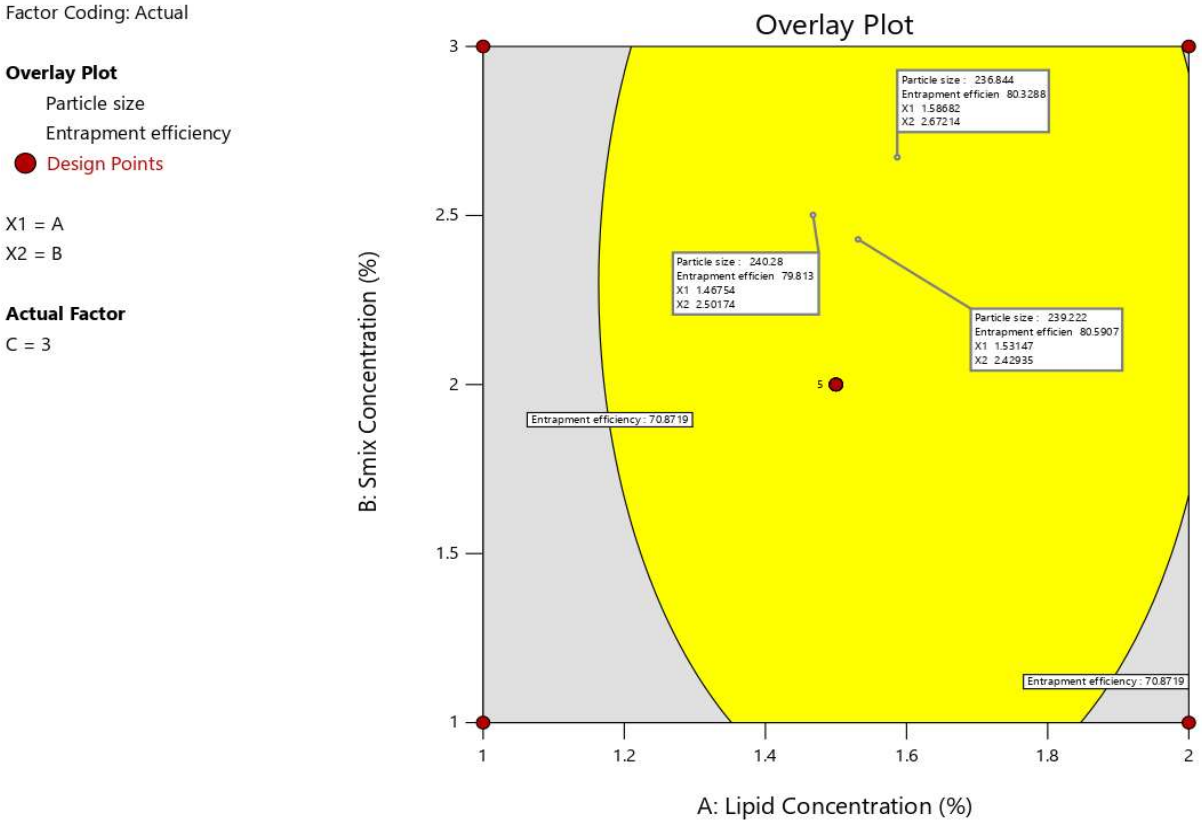

Figure 6.16 Overlay plot for optimization of LZ NLCs

Table 6.14: Results of check point batch and optimized batch for particle size and %EE

Batch	X1 (%Lipid Concentration)	X2 (%S_{mix} Concentration)	X3 (Sonication time)	Y1 (Particle Size)	Y2 (%EE)	Predicated Y1 (Particle Size)	Predicated Y2 (%EE)
Check point 1	1.59	2.67	3	236.37	80.73	236.84	80.33
Check point 2	1.47	2.50	3	240.02	79.61	240.28	79.81
Check point 3	1.53	2.43	3	240.03	80.05	239.22	80.59

A checkpoint analysis was performed to confirm the role of the derived polynomial equation and contour plots in predicting the responses.

6.4.3 Formulation optimization by Box-Behnken Design for Tavaborole loaded NLCs

Based on the preliminary investigation, three CMA were identified, and their relationship with CQA was exhaustively investigated using Box-Behnken Design. A randomized matrix of 17 runs was generated by Design-Expert software and presented in below Table 6.15.

Table 6.15: Randomized BBD design matrix generated Design-Expert software

Run	Independent Variables			Dependent Variables (CQA)	
	A:Lipid concentration (%)	B:Smix Concentration (%)	C:Sonication time (Min)	Particle size (nm)	% EE
1	1.5	2	3	243.34±0.87	78.82±1.04
2	2	3	3	238.01±0.54	70.04±0.07
3	1	3	3	230.96±1.02	60.52±0.63
4	1.5	1	2	258.00±0.28	68.82±0.09
5	1.5	1	4	198.91±0.07	71.28±0.41
6	1.5	2	3	237.32±0.94	80.09±0.26

7	1	2	4	201.37±0.55	59.92±0.06
8	2	2	2	260.00±1.36	71.33±1.03
9	2	1	3	238.12±0.06	71.93±0.29
10	1	2	2	255.51±0.83	63.91±0.33
11	1.5	2	3	240.00±0.07	80.59±0.91
12	1	1	3	239.33±1.18	50.03±1.06
13	1.5	3	4	190.06±0.51	73.65±1.27
14	1.5	2	3	239.39±0.36	79.98±0.61
15	2	2	4	199.00±1.05	76.93±1.04
16	1.5	2	3	242.22±0.51	80.71±0.39
17	1.5	3	2	265.41±0.37	76.41±1.64

6.4.3.1 Effect analysis of critical variables on responses

6.4.3.1.1 Influence of investigated parameters on Particle size

A) Statistical Analysis for Particle size

The statistical analysis of the design mentioned above is as follows:

Table 6.16 Statistical analysis of design for Particle size

Source	Sequential p-value	Lack of Fit p-value	Adjusted R^2	Predicted R^2	
Linear	< 0.0001	0.0141	0.9060	0.8671	
2FI	0.6727	0.0094	0.8945	0.7734	
Quadratic	**0.0027**	**0.1284**	**0.9777**	**0.8827**	**Suggested**
Cubic	0.1284		0.9893		**Aliased**

As shown in table 6.13, the best model to fit the experimental results of Particle size in NLCs is the quadratic model and was chosen for further evaluation.

B**) ANOVA Analysis for Particle size**

The ANOVA for Particle size is given in below table 6.17**.**

Table 6.17 ANOVA for Response Surface Quadratic Model for Particle size

Source	**Sum of Squares**	**df**	**Mean Square**	**F- value**	**p-value**	
Model	8403.08	9	933.68	78.93	< 0.0001	Significant
A-Lipid Concentration	12.50	1	12.50	1.06	0.3382	
B-Smix Concentration	12.50	1	12.50	1.06	0.3382	
C-Sonication time	7812.50	1	7812.50	660.48	< 0.0001	
AB	20.25	1	20.25	1.71	0.2321	
AC	12.25	1	12.25	1.04	0.3427	
BC	56.25	1	56.25	4.76	0.0656	
A^2	9.16	1	9.16	0.7744	0.4080	
B^2	25.79	1	25.79	2.18	0.1833	
C^2	418.95	1	418.95	35.42	0.0006	
Residual	82.80	7	11.83			
Lack of Fit	60.00	3	20.00	3.51	0.1284	not significant
Pure Error	22.80	4	5.70			
Cor Total	8485.88	16				

The model is significant, according to the model's F-value of 78.93. The high F value has a 0.01% probability of being caused by noise. Model terms are considered significant when P-values are less than 0.0500. C and C^2 are important model terms in this instance. The model terms are not important if the value is bigger than 0.1000. Reducing the number of insignificant model terms (excluding those necessary for hierarchy) could potentially enhance the model. When compared to the pure mistake, the Lack of Fit appears to be insignificant, as indicated by

the 3.51 Lack of Fit F-value. A significant F-value for Lack of Fit could be the result of noise, with a 12.84% probability. Fit is desirable; a non-significant deficiency in fit is desirable.

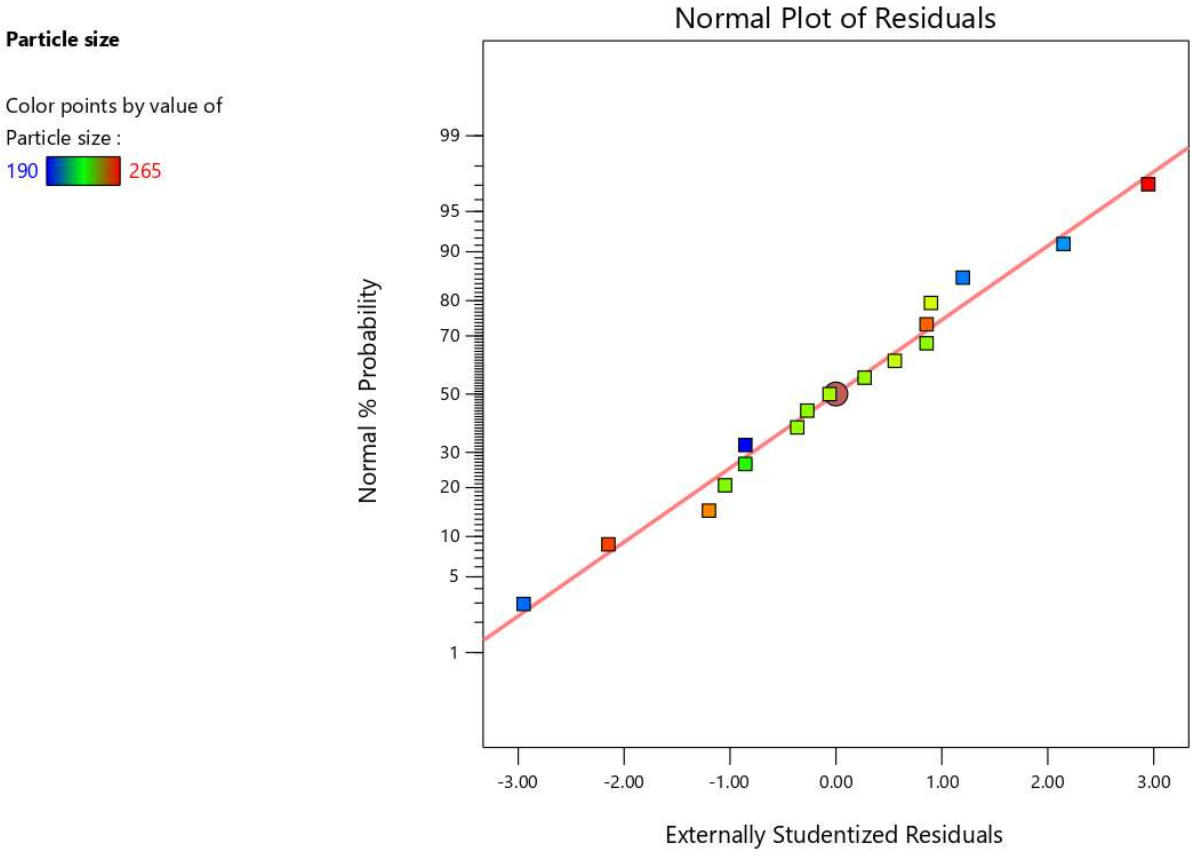

Figure 6.17 Actual v/s Predicted plot for % Particle size

Table 6.18 ANOVA study results for Particle size

Parameters Results of Response	Parameters Results of Response
Std Deviation	3.44
Mean	233.65
C.V.%	1.47
R-Squared	0.9902
Adjusted R-Squared	0.9777
Predicted R-Squared	0.8827
Adeq. Precision	27.1059

There is less than 0.2 discrepancy between the Adjusted R^2 of 0.9777 and the Predicted R^2 of 0.8827, indicating a satisfactory agreement. Adeq Precision calculates the ratio of signal to noise. Ideally, the ratio should be higher than 4. With a ratio of 27.106, signal strength is sufficient. The design area can be navigated with the help of this model.

C) Mathematical Model for Particle size

In addition to the ANOVA value, contour plots and three-dimensional plots were used to investigate the impact of different factors on particle size. Table 5.15 shows that the ultimate reaction, or particle size, confirms the influence of different components when the combination of different degrees of factors changes. Examining the various contributing factors in detail helps us to better grasp the magnitude of the effect. Positive and negative effects are discussed in the equation.

The final equation in terms of coded factors:

Particle size:

$+240.20+1.25*A+1.20*B- 31.25*C+2.25*AB-1.75*AC-3.75*BC-1.47*A^2-2.47*B^2-9.98*C^2$

Table 6.19: The Final equation in terms of actual factors

Particle Size	=
+240.20	
+1.25	Lipid Concentration
+1.20	S_{mix} Concentration
- 31.25	Sonication time
+2.25	Lipid Concentration * S_{mix} Concentration
-1.75	Lipid Concentration * Sonication time
-3.75	S_{mix} Concentration * Sonication time
-1.47	Lipid Concentration^2
-2.47	S_{mix} Concentration^2
-9.98	Sonication time^2

The presence of a positive sign preceding a factor signifies an increase in response with the factor and vice versa. Furthermore, it can be seen from the preceding equation that each element

has some effect on particle size. Two of the three independent variables that were selected have positive effects on particle size and one of the three independent variables that were selected have negative effects on particle size as shown by the coefficient values of the individual factors. The highest co-efficient value before factor C indicates that sonication time has the greatest impact on particle size, which is followed by lipid concentration and S_{mix} Concentration. As an example, particle size increases when lipid concentration increases. An increase in sonication time was shown to cause a decrease in particle size. It may be because of the disruption of the particles caused by an increase time of sonication (29).

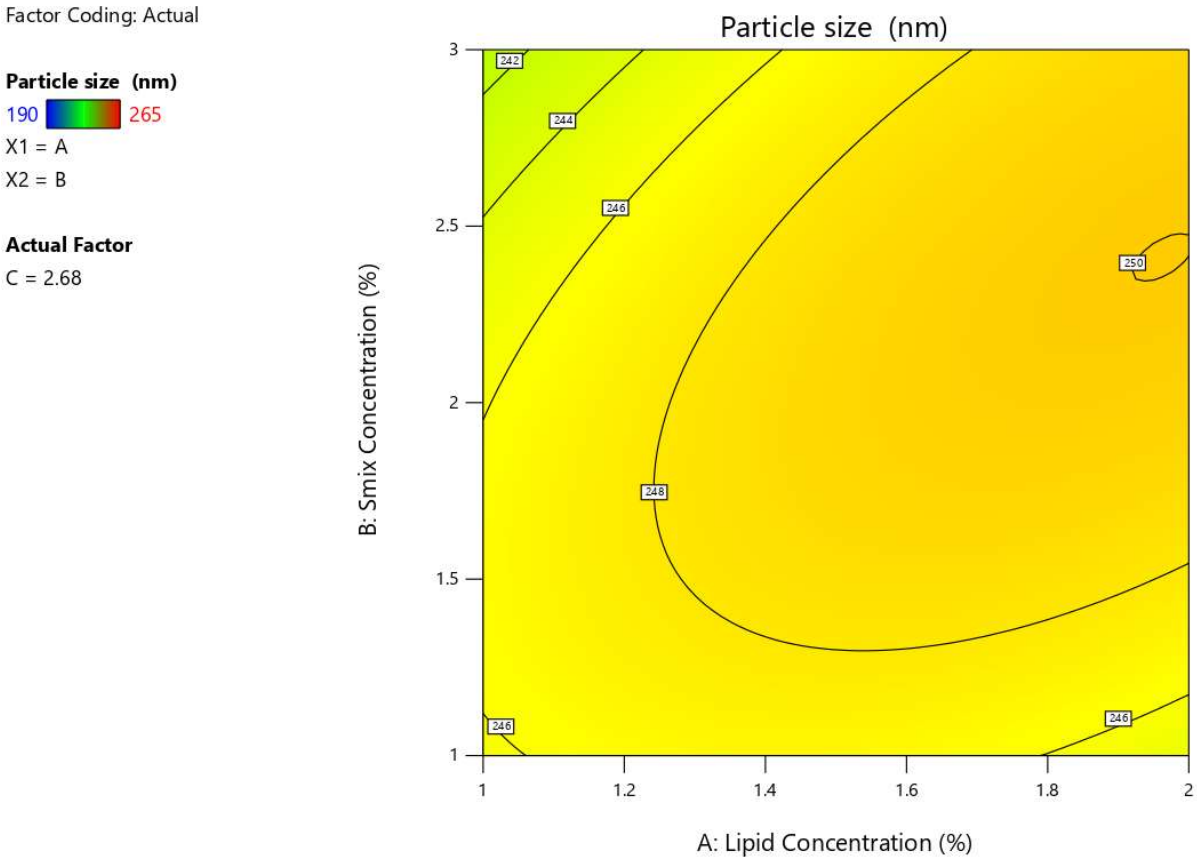

Figure 6.18 Contour plot (2D) showing the combined effect of lipid concentration and Smix concentration on Particle size

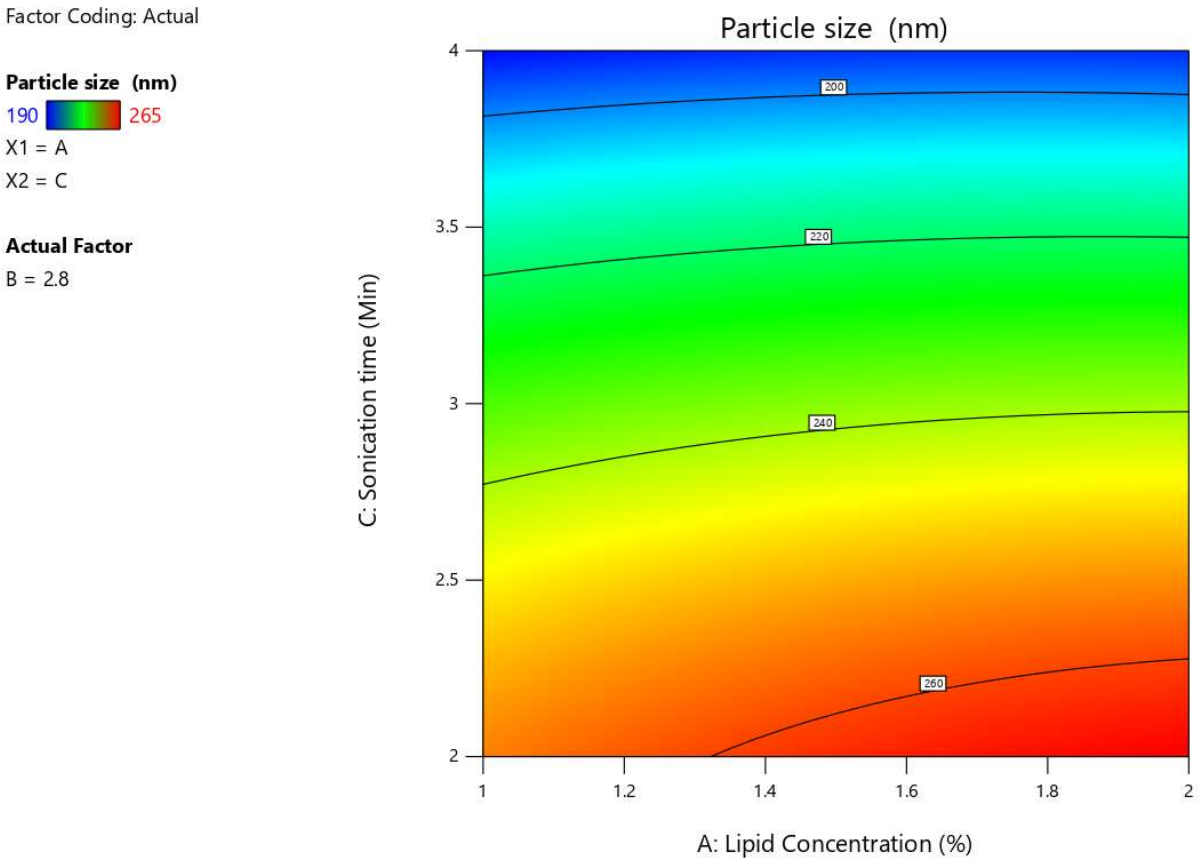

Figure 6.19 Contour plot (2D) showing the combined effect of lipid concentration and sonication time on Particle size

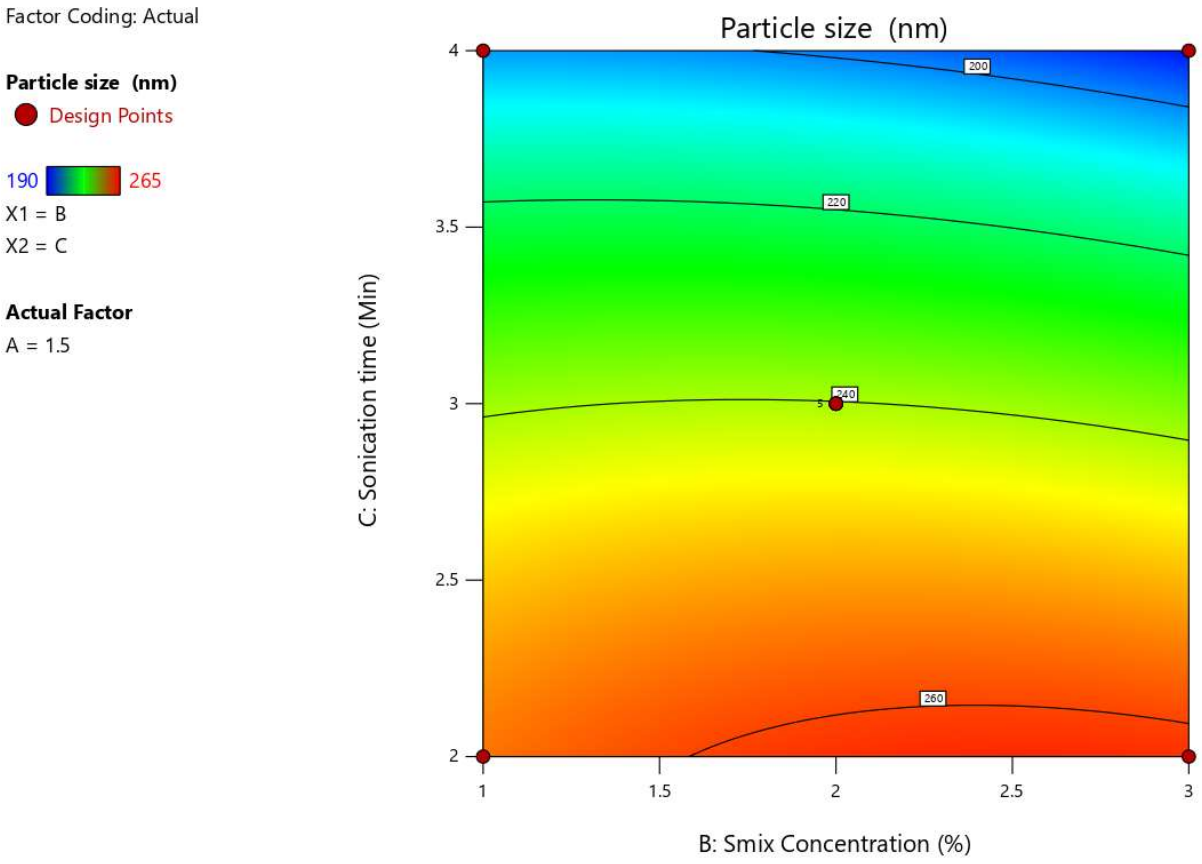

Figure 6.20 Contour plot (2D) showing the combined effect of Sonication time and Smix concentration on Particle size

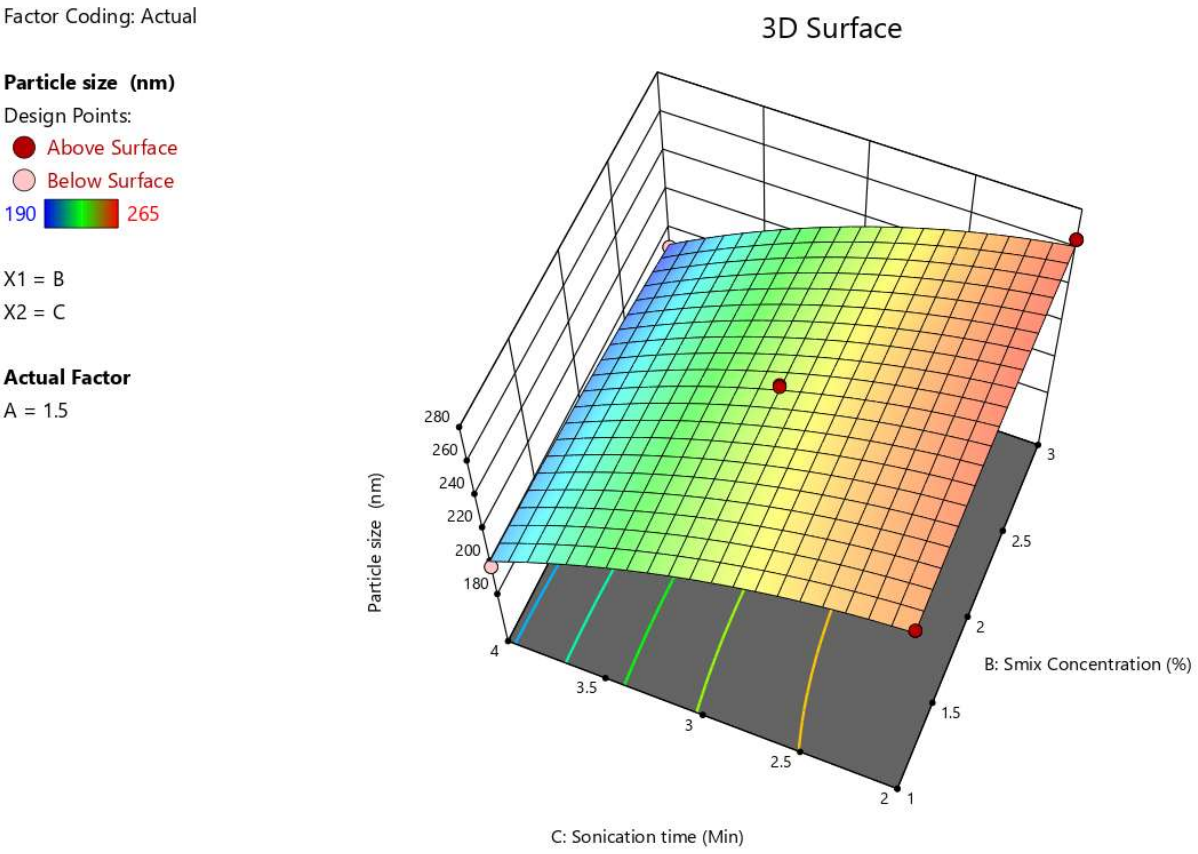

Figure 6.21 Response surface (3D) showing the combined effect of Smix concentration and Sonication time on Particle size

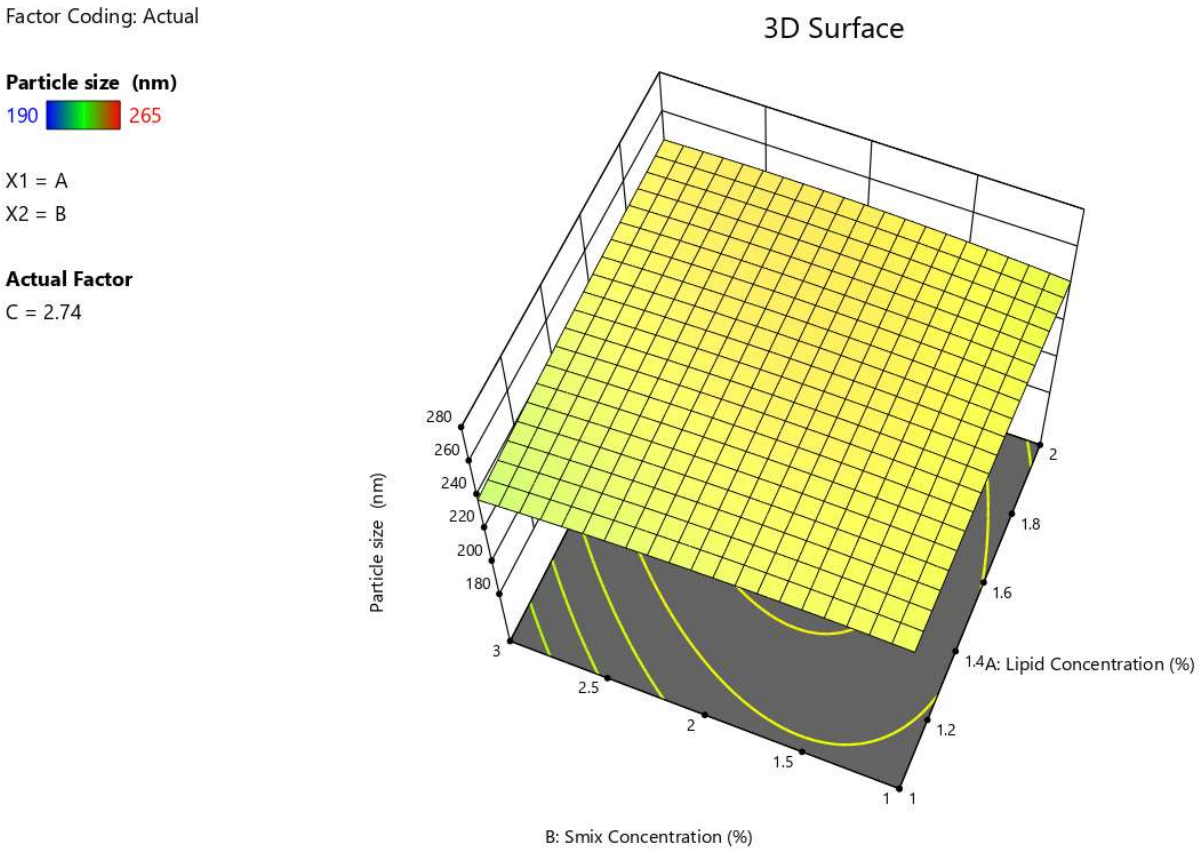

Figure 6.22 3D surface graph showing the combined effect of lipid concentration and Smix concentration on Particle size

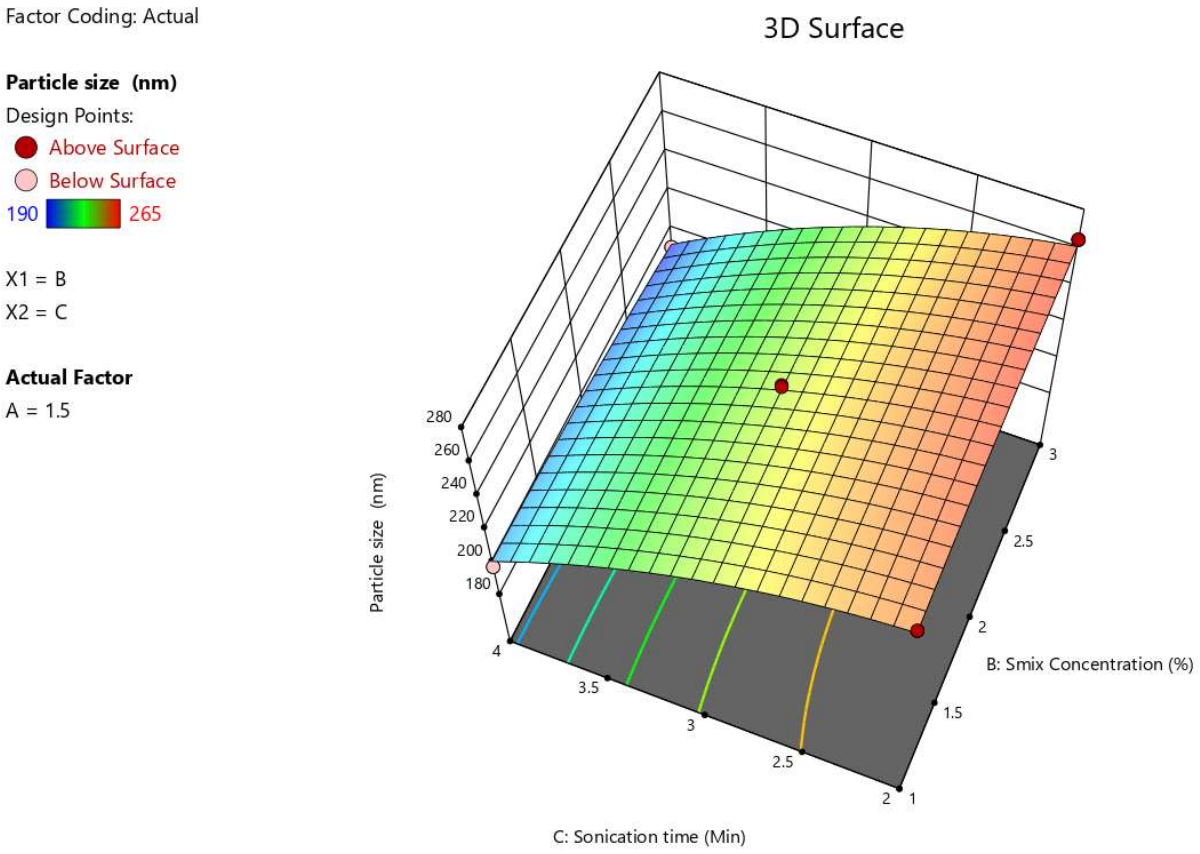

Figure 6.23 3D surface graph showing the combined effect of Lipid concentration and sonication time on Particle size

The effects of independent factors on the particle size are shown in figure 6.18 to figure 6.23. The largest particle size is shown by the red area, and the lowest particle size is represented by the blue zone. It can be depicted that particle size increases when lipid concentration and S_{mix} increases and particle size decreases as sonication time increases (30). These graphs show the relationship between the CQA and the corresponding independent factor while maintaining constant levels of the other independent variables.

6.4.3.1.2 Influence of investigated parameters on % EE

A) Statistical Analysis for % EE

The statistical analysis of the design mentioned above is as follows:

Table 6.20 Statistical analysis of design for % EE

Source	Sequential p-value	Lack of Fit p-value	Adjusted R^2	Predicted R^2	
Linear	0.1125	0.0001	0.2107	-0.0475	
2FI	0.8099	< 0.0001	0.0641	-0.7789	
Quadratic	**< 0.0001**	**0.1056**	**0.9829**	**0.9071**	**Suggested**
Cubic	0.1056		0.9926		**Aliased**

As shown in table 6.20, the best model to fit the experimental results of % EE in NLCs is the quadratic model and was chosen for further evaluation.

B) ANOVA Analysis for % EE

The ANOVA for Particle size is given in below table.

Table 6.21 ANOVA for Response Surface Quadratic Model for % EE

Source	Sum of Squares	df	Mean Square	F- value	p-value	
Model	1198.69	9	133.19	103.13	< 0.0001	Significant
A-Lipid Concentration	389.90	1	389.90	301.90	< 0.0001	
B-Smix Concentration	43.06	1	43.06	33.34	0.0007	
C-Sonication time	0.2145	1	0.2145	0.1661	0.6958	
AB	38.32	1	38.32	29.67	0.0010	
AC	22.99	1	22.99	17.80	0.0039	
BC	6.81	1	6.81	5.27	0.0553	
A^2	483.21	1	483.21	374.14	< 0.0001	

B^2	161.60	1	161.60	125.13	< 0.0001	
C^2	7.15	1	7.15	5.53	0.0509	
Residual	9.04	7	1.29			
Lack of Fit	6.79	3	2.26	4.03	0.1056	not significant
Pure Error	2.25	4	0.5615			
Cor Total	1207.73	16				

The model is significant, according to the model's F-value of 103.13. The high F-value has a 0.01% probability of being caused by noise. Model terms are considered significant when P-values are less than 0.0500. A, B, AB, AC, A^2, and B^2 are important model terms in this instance. The model terms are not important if the value is bigger than 0.1000. Reducing the number of insignificant model terms (excluding those necessary for hierarchy) could potentially enhance the model. In comparison to the pure mistake, the Lack of Fit appears to be insignificant, as indicated by the F-value of 4.03. An F-value for Lack of Fit this large could be the result of noise with a 10.56% probability. Fit is desirable; a non-significant deficiency in fit is desirable.

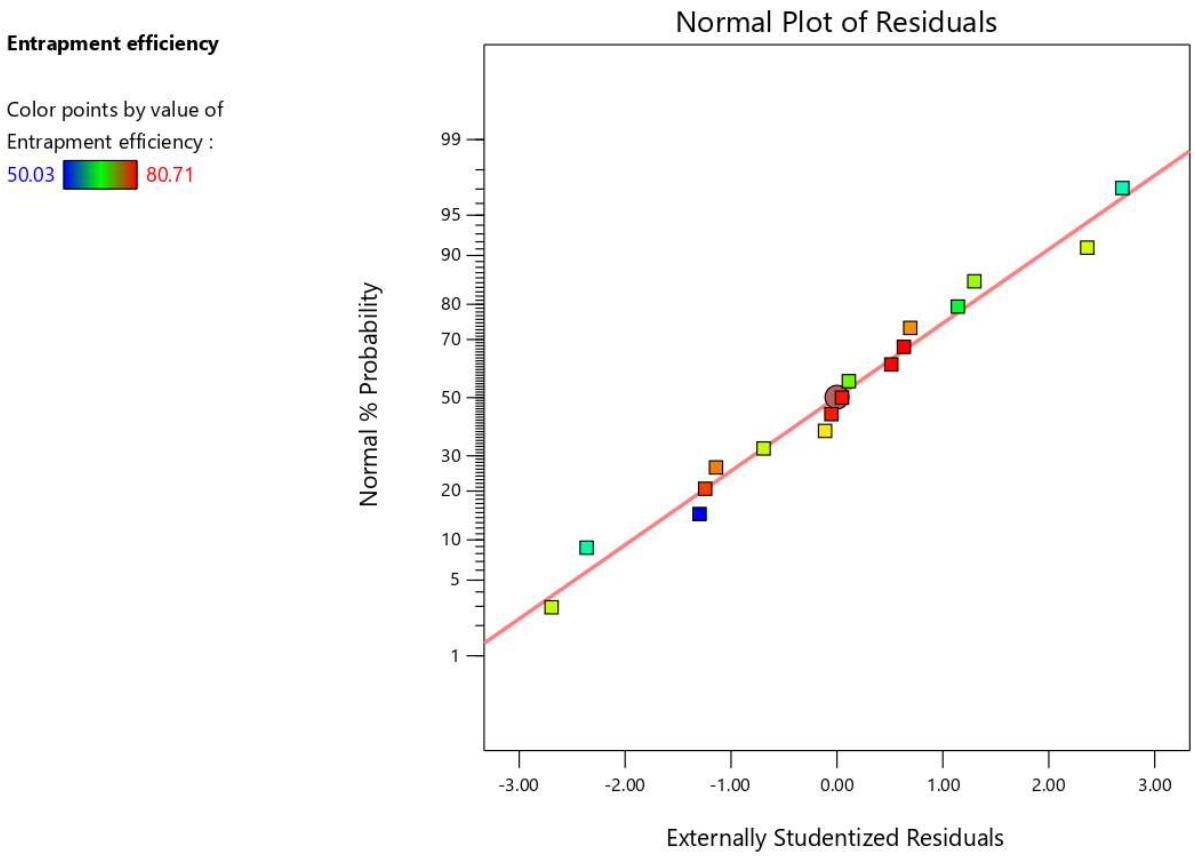

Figure 6.24 Actual v/s Predicted plot for % EE

Table 6.22 ANOVA study results for % EE

Parameters Results of Response	Parameters Results of Response
Std Deviation	1.14
Mean	71.47
C.V.%	1.59
R-Squared	0.9925
Adjusted R-Squared	0.9829
Predicted R-Squared	0.9071
Adeq. Precision	33.6206

The Adjusted R^2 of 0.9829 and the Predicted R^2 of 0.9071 are reasonably in agreement with one another; that is, the difference is less than 0.2. Adeq Precision calculates the ratio of signal to

noise. Ideally, the ratio should be higher than 4. With a ratio of 33.621, signal strength is sufficient. The design area can be navigated with the help of this model.

C) Mathematical Model for % EE:

Contour plots and the 3D plot were used in conjunction with the ANOVA value to investigate the impact of different factors on the percentage of % EE. Table 6.18 shows that the final response, or % EE, confirms the impact of different factors when the combination of different amounts of factors changes. Examining the various contributing factors in detail helps us to better grasp the magnitude of the effect. Positive and negative effects are discussed in the equation.

The final equation in terms of coded factors:

% EE: $+80.04+6.98*A+0.4232*B-0.1638*C-3.09*AB+2.40*AC-1.30*BC-10.71*A^2-4.620*B^2-1.30*C^2$

Table 6.23 The Final equation in terms of actual factors

% EE	**=**
+80.04	
+6.98	Lipid Concentration
+0.4232	S_{mix} Concentration
-0.1638	Sonication time
-3.09	Lipid Concentration * S_{mix} Concentration
+2.40	Lipid Concentration * Sonication time
-1.30	S_{mix} Concentration * Sonication time
-10.71	Lipid Concentration^2
-4. 620	S_{mix} Concentration^2
-1.30	Sonication time^2

The presence of a positive sign preceding a factor signifies an increase in response with the factor and vice versa. Furthermore, it can be seen from the preceding equation that each element has some effect on %EE. Two of the three independent variables that were selected have positive effects on %EE and one of the three independent variables that were selected have negative effects on %EE as shown by the coefficient values of the individual factors. As an example, % EE increases when lipid concentration increases. API partitioned into the lipidic phase, resulting

in an increase in % EE with an increase in lipid concentration. An increase in sonication time was shown to cause a decrease in % EE (29).

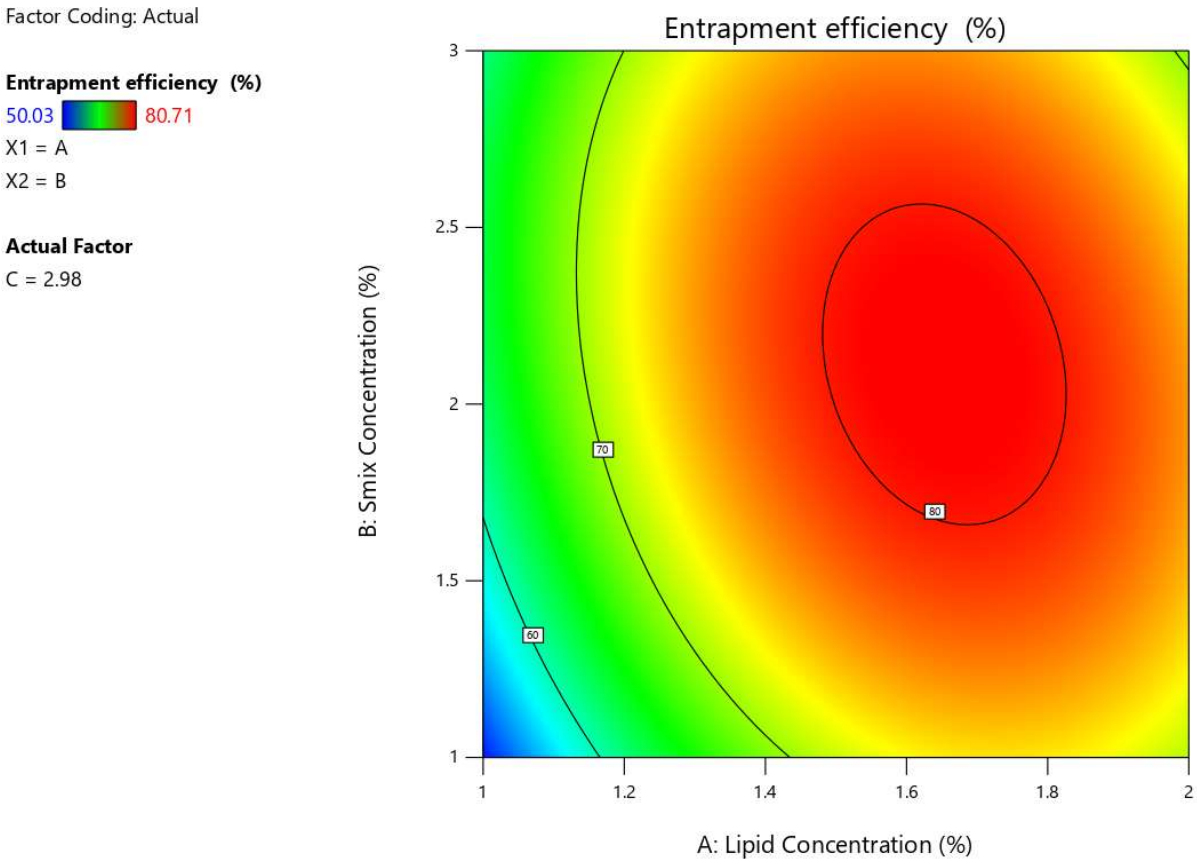

Figure 6.25 Contour plot (2D) showing the combined effect of Lipid concentration and Smix Concentration on % EE

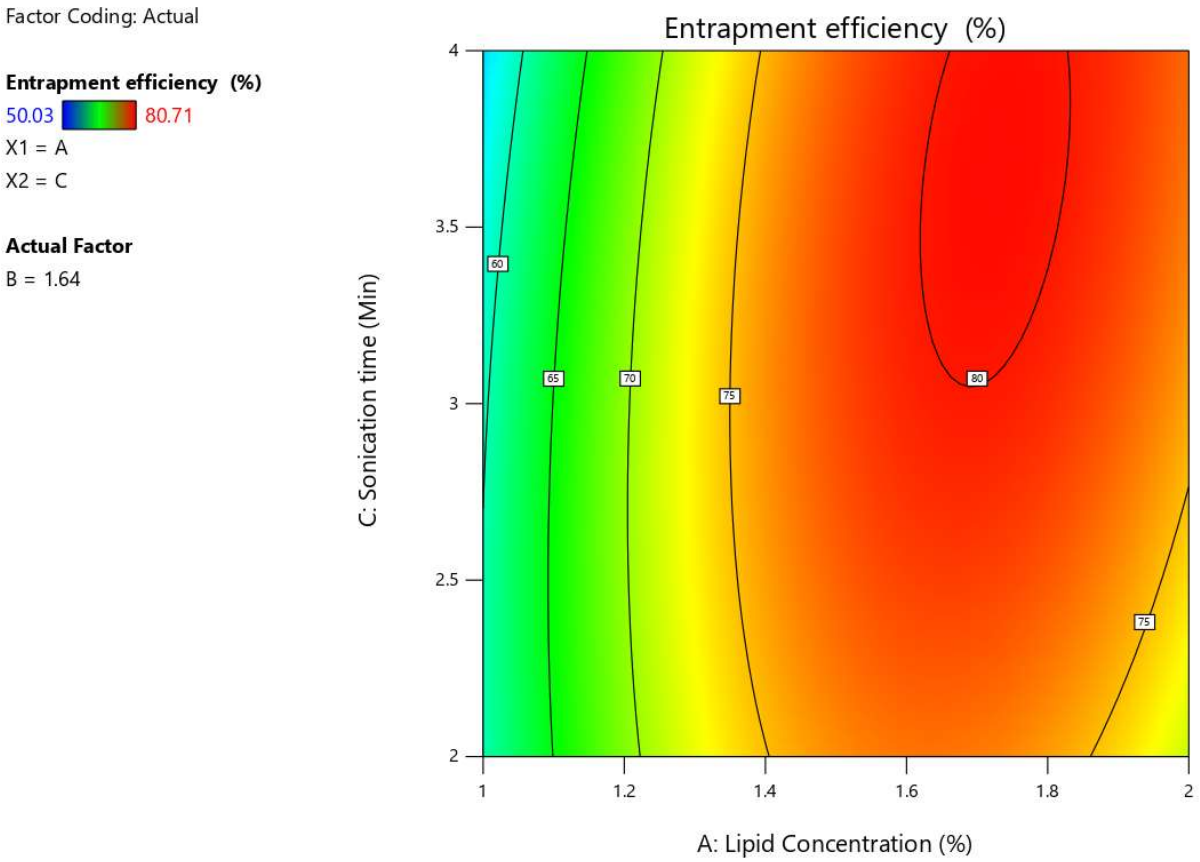

Figure 6.26 Contour plot (2D) showing the combined effect of Lipid concentration and Sonication time on % EE

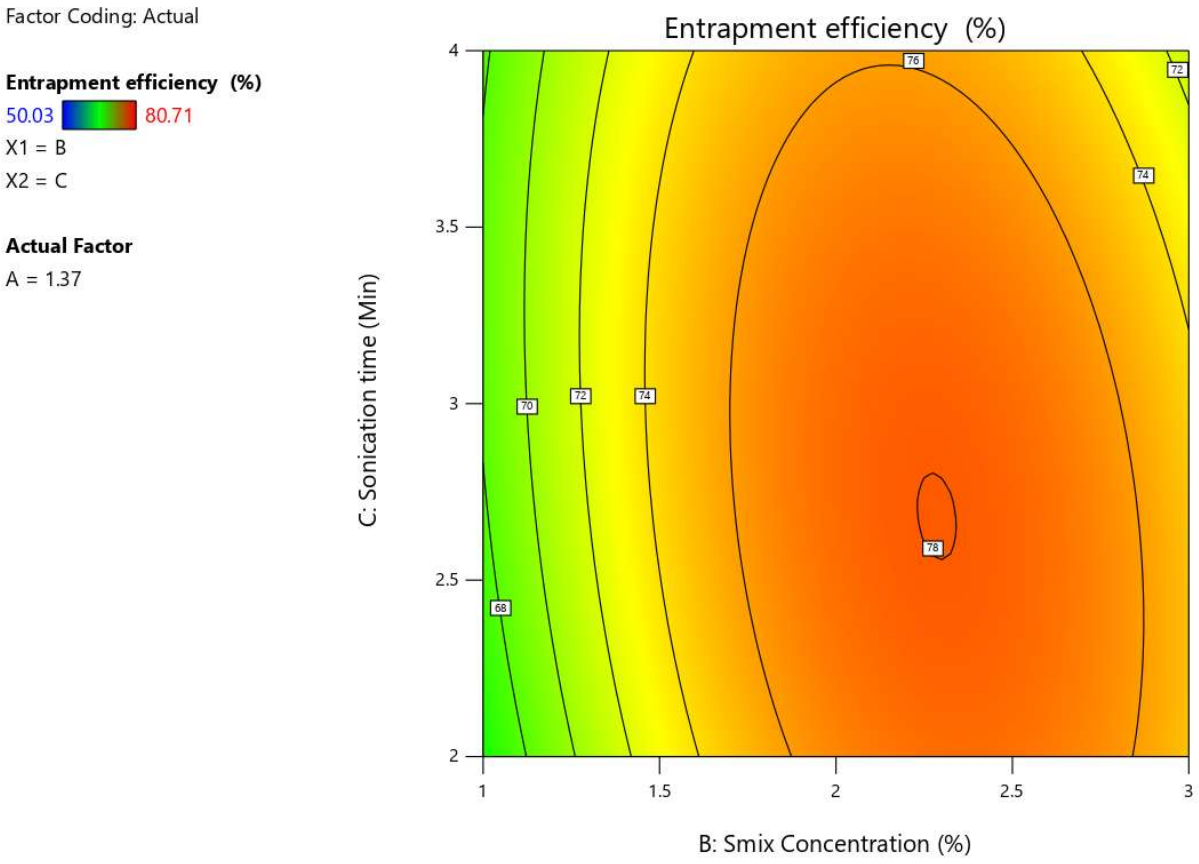

Figure 6.27 Contour plot (2D) showing the combined effect of Smix concentration and Sonication time on % EE

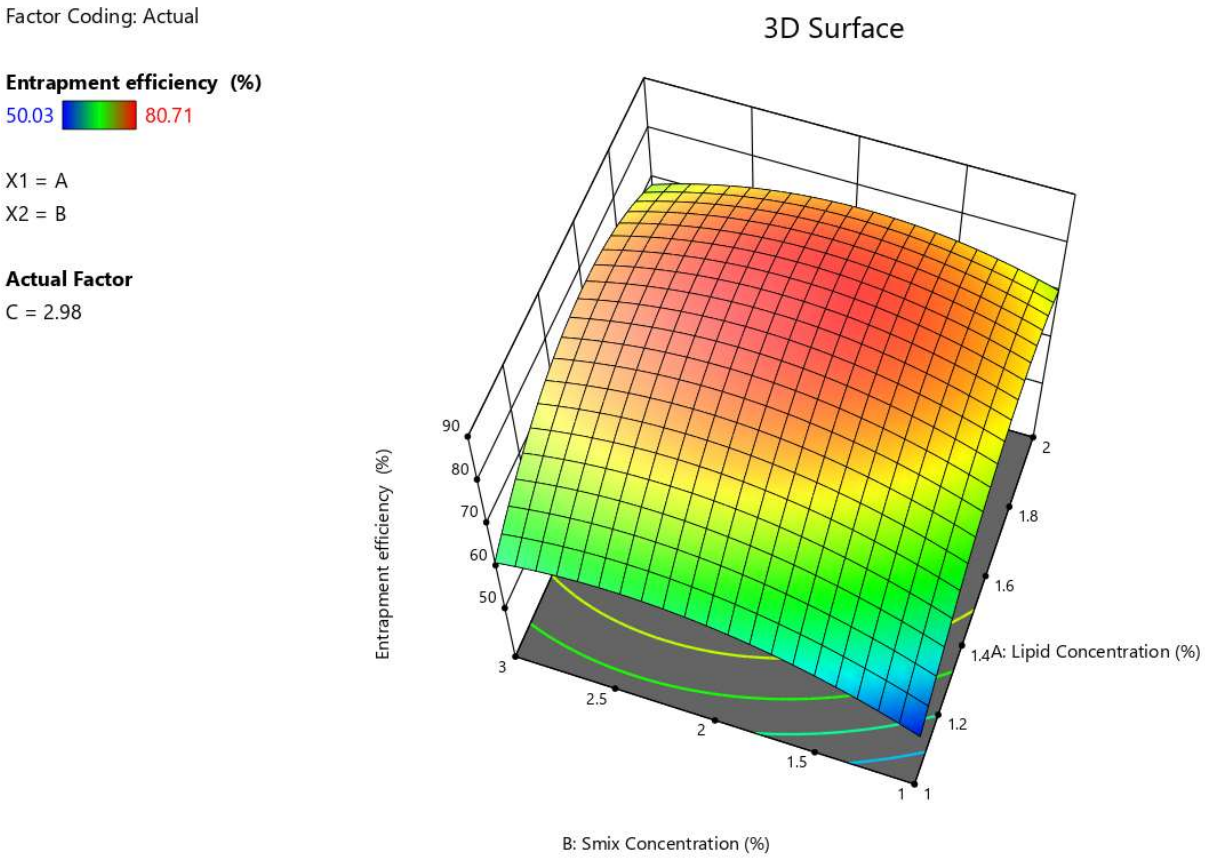

Figure 6.28 Response surface (3D) showing the combined effect of lipid concentration and Smix concentration on % EE

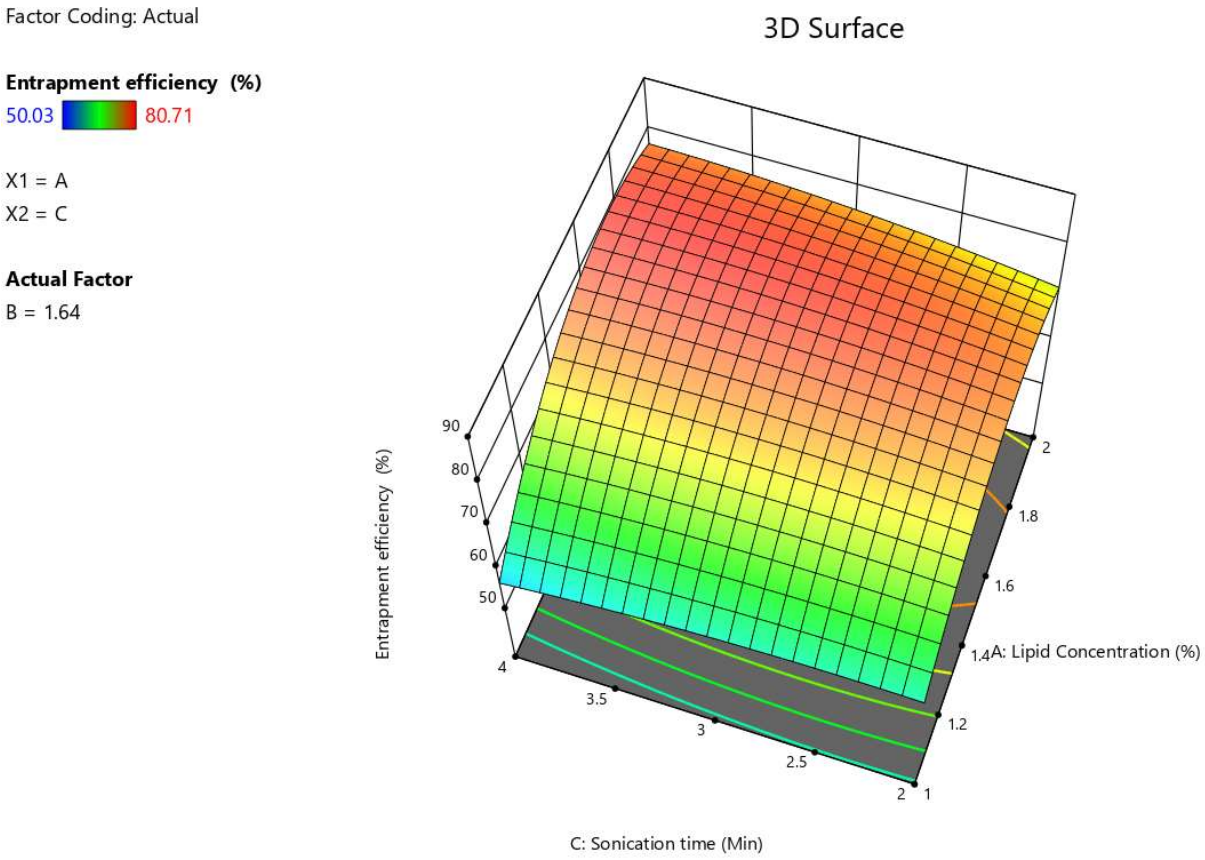

Figure 6.29 Response surface (3D) showing the combined effect of lipid concentration and Sonication time on % EE

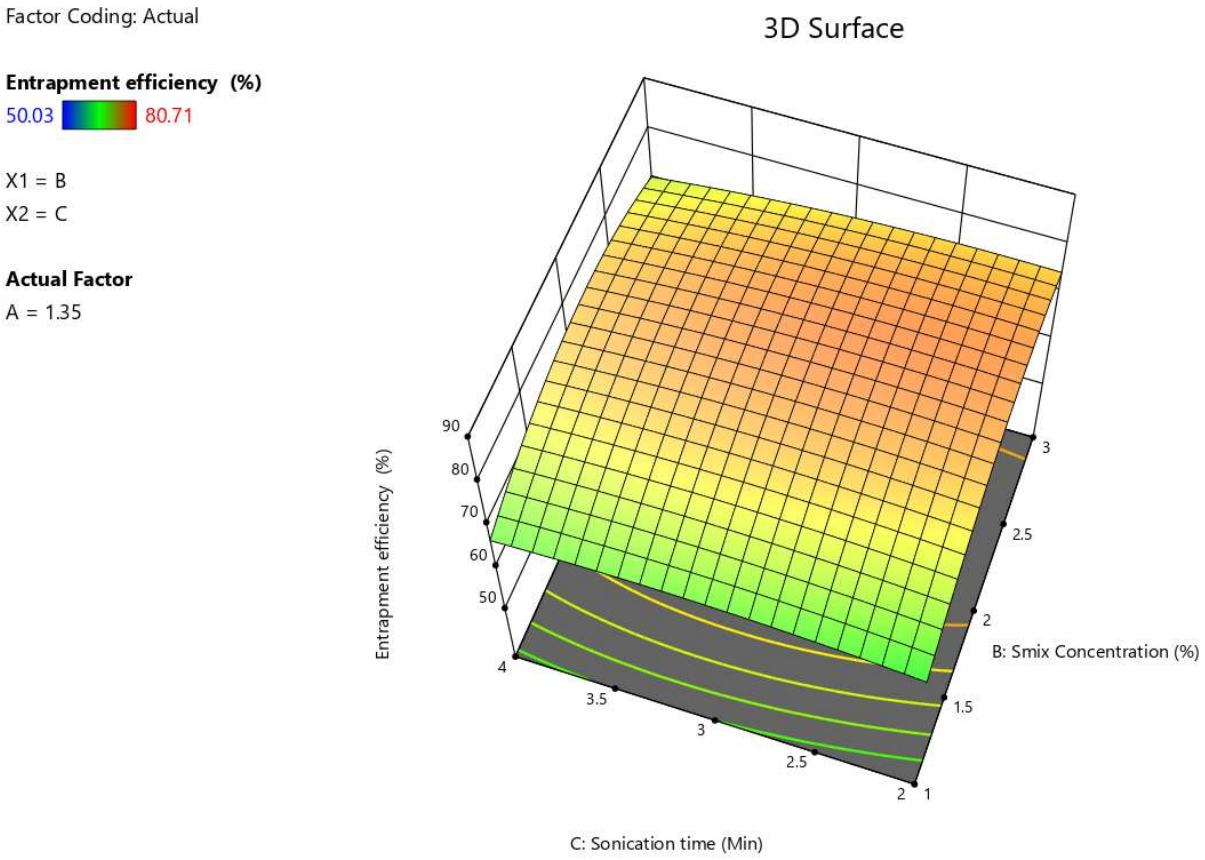

Figure 6.30 Response surface (3D) showing the combined effect of Smix concentration and Sonication time on % EE

The effects of independent factors on the % EE are shown in figure 6.24 to figure 6.30. The highest % EE is shown by the red area, and the lowest % EE is represented by the blue zone. It can be depicted that % EE increases when lipid concentration and S_{mix} concentration increases. An increase in sonication time was shown to cause a decrease in % EE (30). These graphs show the relationship between the CQA and the corresponding independent factor while maintaining constant levels of the other independent variables.

6.5.3.2 Preparation of checkpoint batches as per the overlay plot

Overlay contour plots for all two CQAs (%EE and particle size) were generated (Fig. 6.31) for obtaining the design space (yellow area in graph).

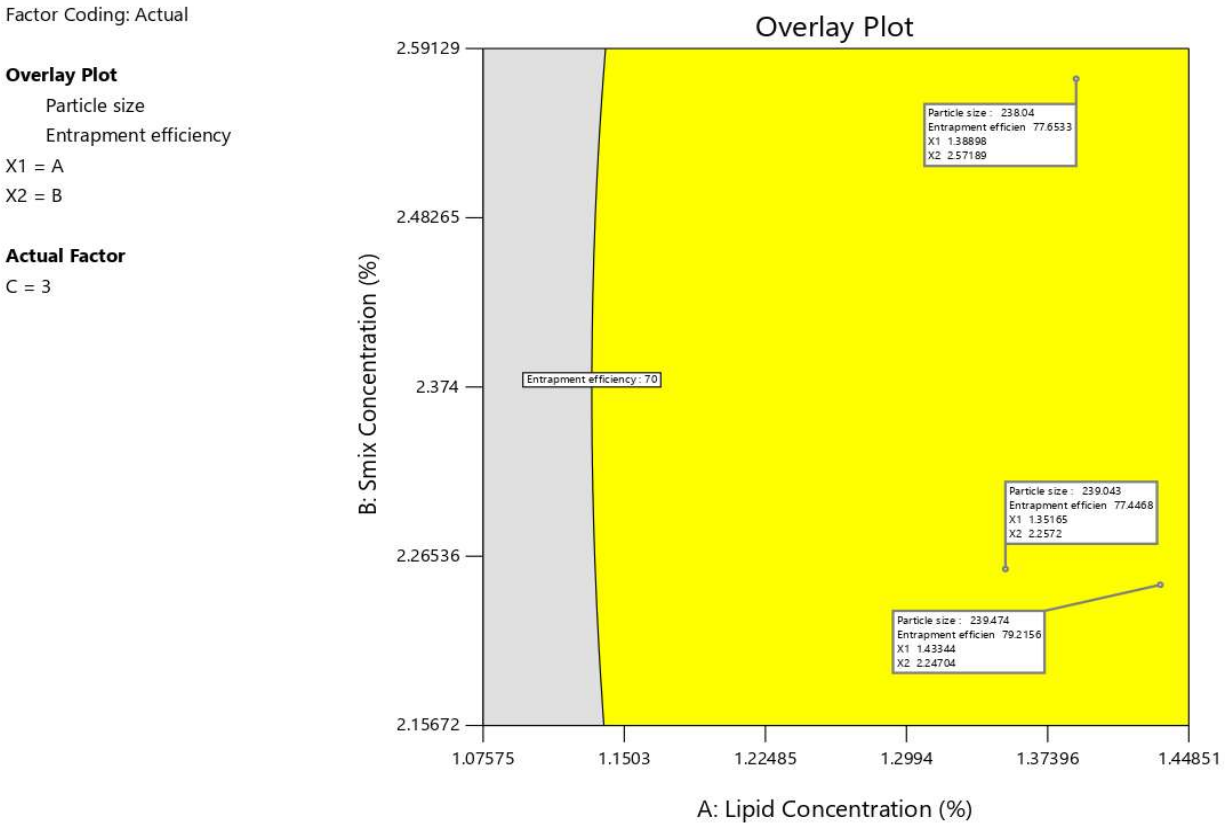

Figure 6.31 Overlay plot of TB NLCs

Table 6.24: Results of check point batch and optimized batch for particle size and %EE

Batch	X1 (%Lipid Concentration)	X2 (%S_{mix} Concentration)	X3 (Sonication time)	Y1 (Particle Size)	Y2 (%EE)	Predicated Y1 (Particle Size)	Predicated Y2 (%EE)
Check point 1	1.39	2.57	3	238.51	77.20	238.04	77.65
Check point 2	1.35	2.26	3	237.28	77.21	237.72	77.45
Check point 3	1.43	2.25	3	239.87	79.08	239.47	79.22

A checkpoint analysis was performed to confirm the role of the derived polynomial equation and contour plots in predicting the responses.

Table 6.25: Composition of optimized batch of LZ NLCs loaded gel and TB NLCs loaded gel

Formulation components	LZ NLCs loaded gel (100 gm)	TB NLCs loaded gel (100 gm)
API	1 gm LZ	5 gm TB
Lipid concentration	1.5 gm Softemul AS	1.5 gm Softemul SE
Smix concentration	2 gm	2 gm
Acetone	3 ml	3 ml
Sonication time	3 min	3 min
Sonication amplitude	40 %	40 %
Carbopol 974 P	1 gm	1 gm
Propylene Glycol	4 gm	4 gm
Triethanolamine	pH adjuster	pH adjuster
Water	87.5 gm	84.5 gm

6.4.4 Characterization of LZ NLCs and TB NLCs:

6.4.4.1 Particle size, PDI, Zeta Potential and %EE:

Particle size of the optimized formulation of LZ NLCs and TB NLCs were found to be 242±1.38 nm and 235±1.44 nm respectively. There was an insignificant difference in the particle size observed in the NLC of Luliconazole and Tavaborole, probably as the excipients and the processing conditions for both the formulations was almost similar. Zeta potential of the optimized formulation of LZ NLCs and TB NLCs were found to be -14.32±1.76 and -23.12±1.43 mV respectively. The measurement of the zeta potential allows to indirectly analyzing the surface charge of the particles and its measurement gives nourishing information about physical stability and mucoadhesive properties of the systems. Zeta potential values of > ±30 mV are generally considered enough for stabilization of NLCs (31). PDI of the optimized formulation of LZ NLCs and TB NLCs were found to be 0.231±1.04 and 0.176±0.52 respectively. The PDI value of developed NLCs is below 0.3 which shows low Polydispersity and acceptable level of homogeneity of developed formulations (32). %EE of the optimized formulation of LZ NLCs and TB NLCs were found to be 80.32±0.41% and 79.98±1.28% respectively. Drug loading of

the optimized formulation of LZ NLCs and TB NLCs were found to be 13.24±0.54% w/w and 11.65±1.87% w/w respectively which indicated that 100 gm of LZ NLCs contains 13.24 gm Luliconazole and 100 gm TB NLCs contains 11.65 gm Tavaborole.

6.4.4.2 Head Space Gas Chromatography (HS-GC) Testing for residual solvent:

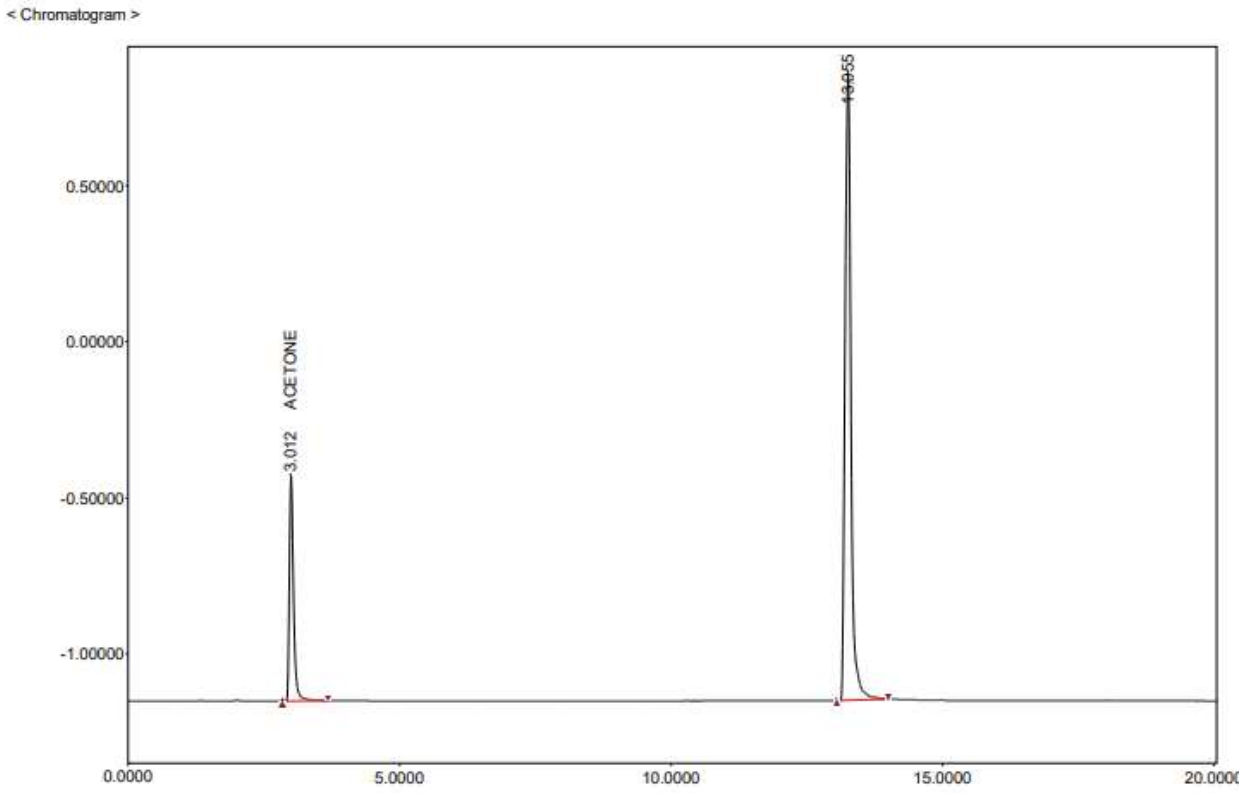

Figure 6.32 GC chromatogram of standard (Acetone)

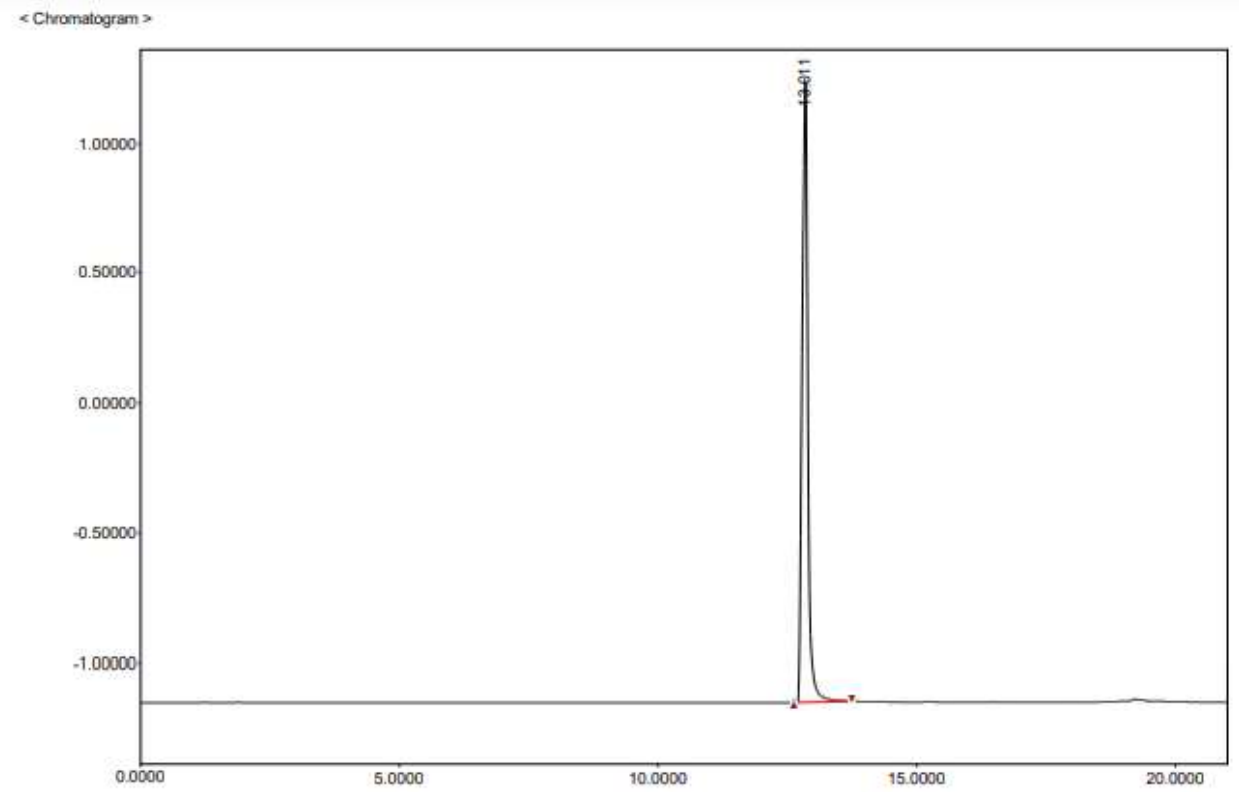

#	RT(min)	Peak name	Area(mV*sec)	Area%
1	13.011		18167.451	100.000

Figure 6.33 GC chromatogram of Luliconazole loaded NLCs

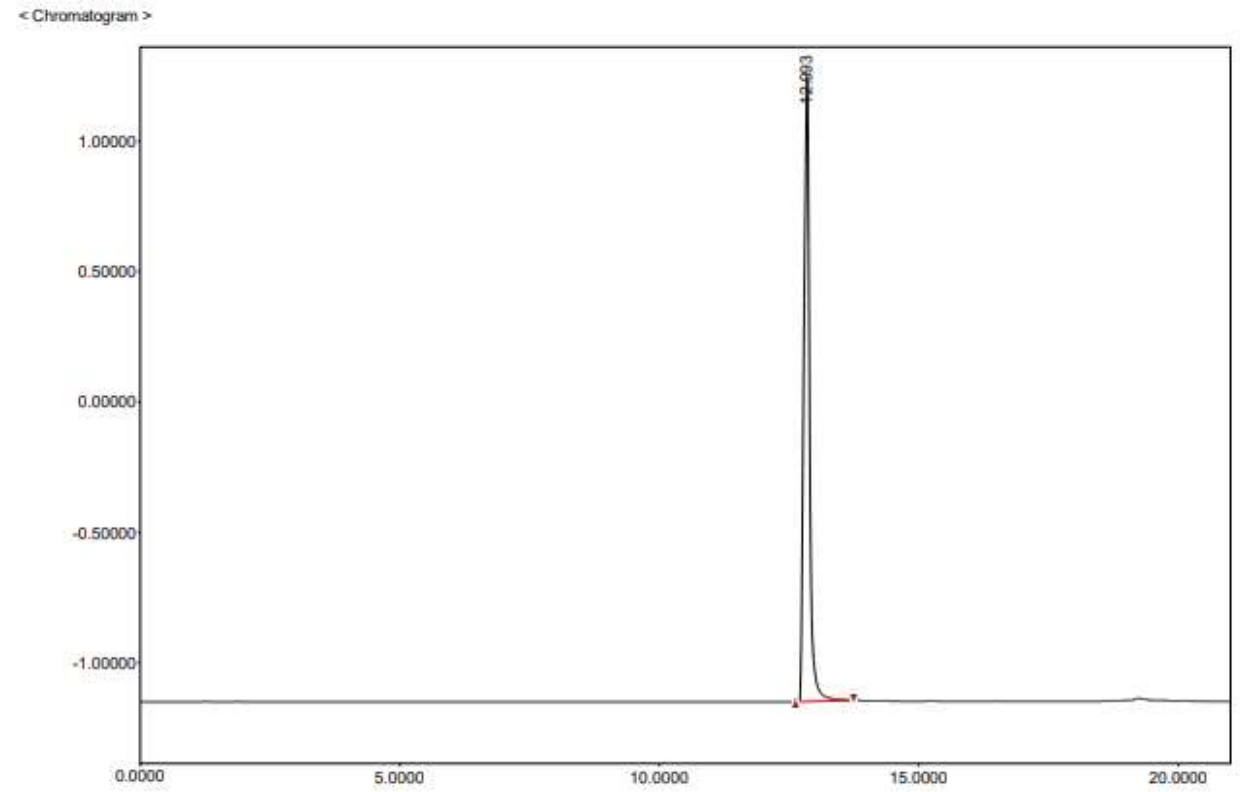

#	RT(min)	Peak name	Area(mV*sec)	Area%
1	12.993		18264.410	100.000

Figure 6.34 GC chromatogram of Tavaborole loaded NLCs

The figure 6.32 shows that retention of peak of acetone is 3.012 which is absent in figure 6.33 and 6.34. Therefore, it can be concluded that acetone is not present in LZ NLCs and TB NLCs.

6.4.4.3 Differential scanning Calorimetry (DSC):

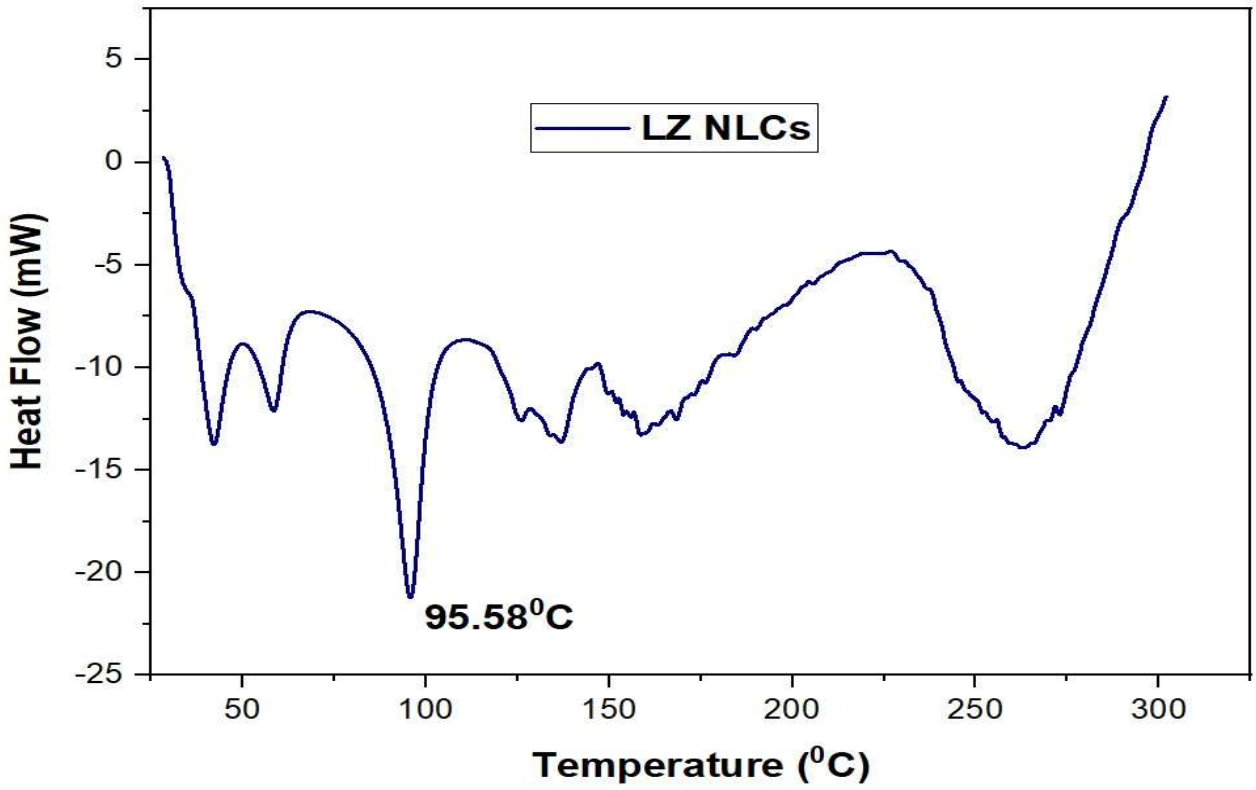

Figure 6.35: DSC graph of Luliconazole loaded NLCs

Figure 6.35 showed the DSC graph of Luliconazole loaded NLCs. It showed the absence of the endothermic drug peak (melting point of Luliconazole 157.89°C – mentioned in figure 4.14 of chapter 4) which indicated successfully incorporation of drug in NLCs matrix.

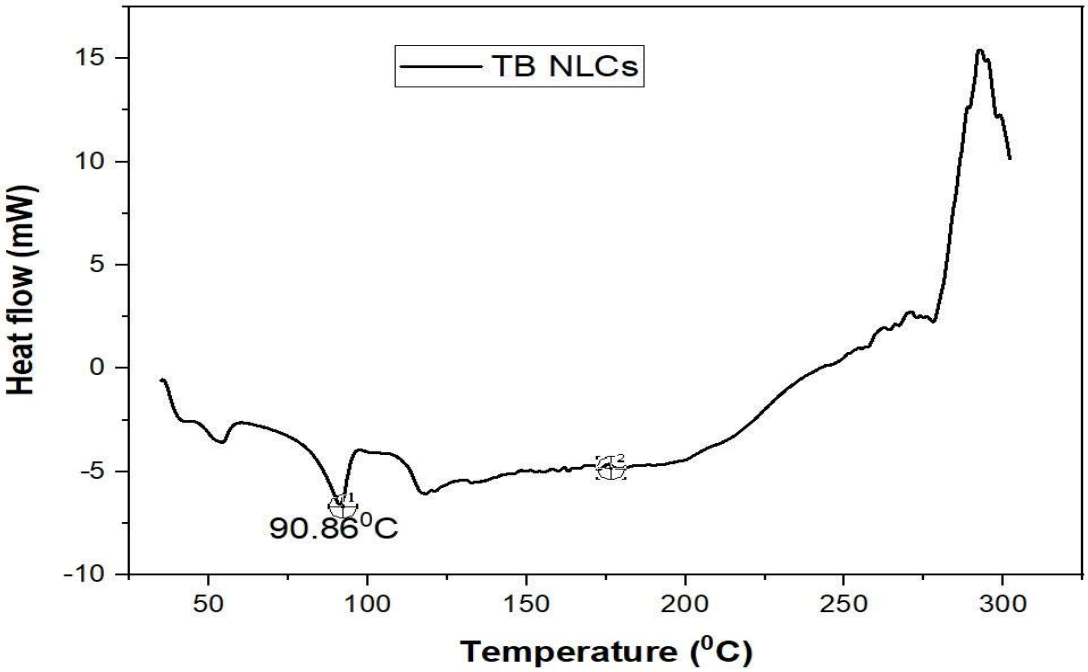

Figure 6.36: DSC graph of Tavaborole loaded NLCs

Figure 6.36 showed the DSC graph of Tavaborole loaded NLCs. It showed the absence of the endothermic drug peak (melting point of Tavaborole 116.16 °C – mentioned in figure 4.15 of chapter 4) which indicated successfully incorporation of drug in NLCs matrix.

6.4.4.4 Transmission electron microscopy (TEM)

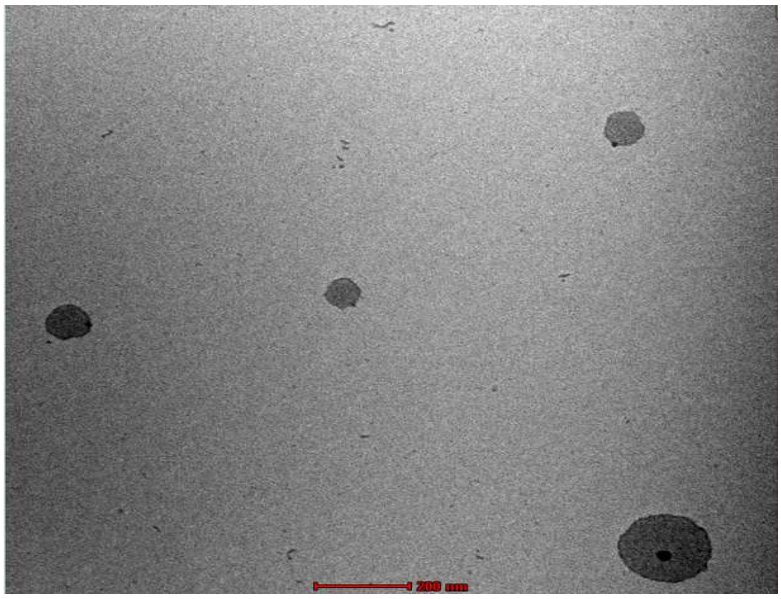

Figure 6.37: TEM image of LZ NLCs

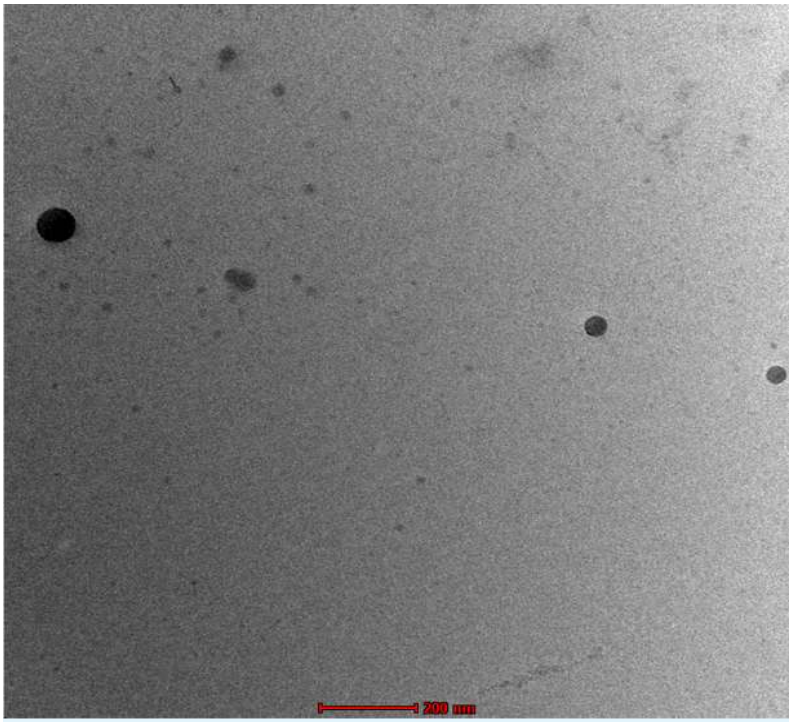

Figure 6.38: TEM image of TB NLCs

Figure 6.37 and figure 6.38 showed TEM images of LZ NLCs and TB NLCs. The morphology of the optimized NLC formulation was observed using TEM. The images demonstrated spherical shapes of the NLCs particles. No aggregation of the particles was observed. TEM analysis also confirmed the nanometric particles diameter of developed formulations (33).

6.4.4.5 Powder X-ray diffraction studies:

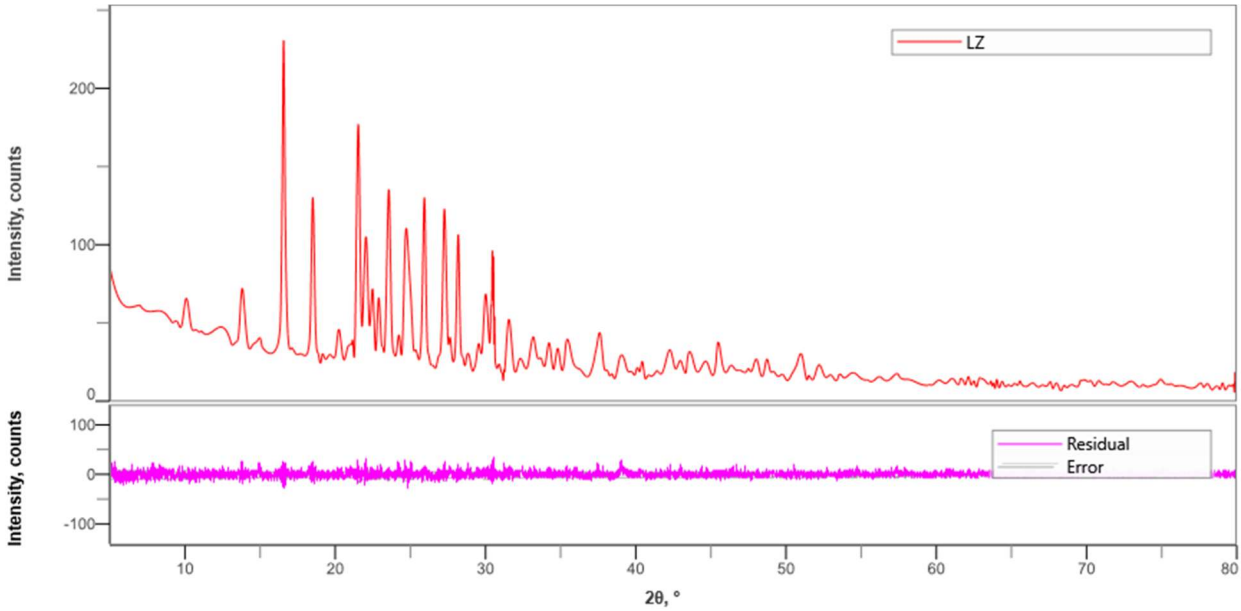

Figure 6.39: XRD spectrum of Luliconazole

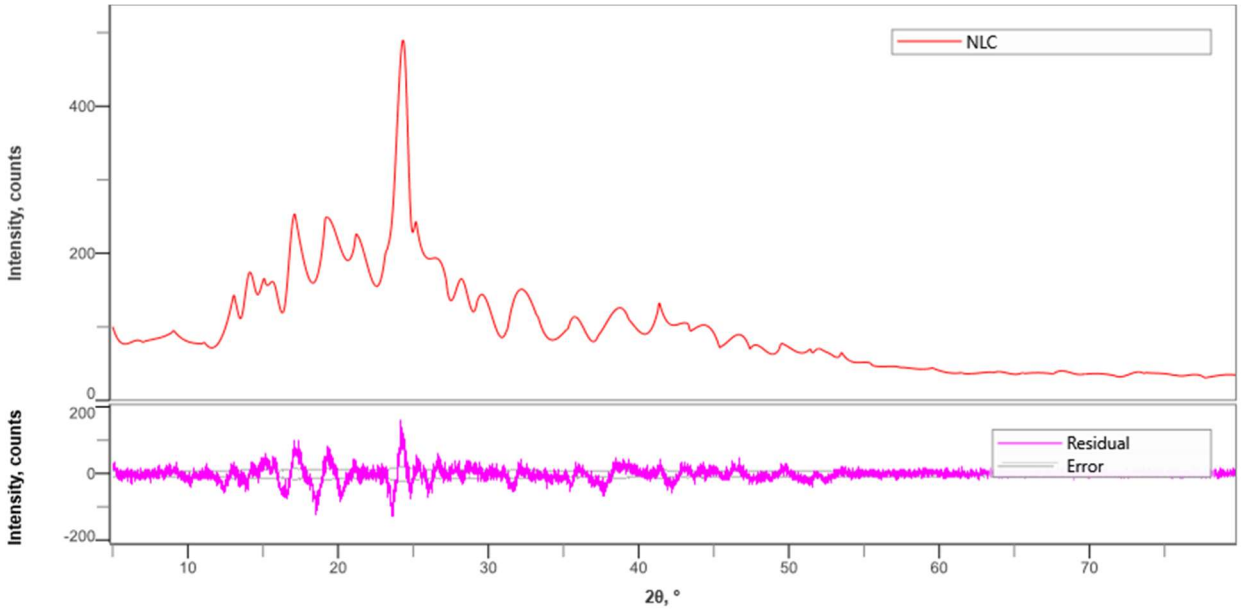

Figure 6.40: XRD spectrum of NLCs of Luliconazole

As shown in figure 6.39 Luliconazole showed intense peaks because of its crystalline structure. Figure 6.40 shows diffraction patterns of NLCs confirmed the transformation of drug from crystalline state to amorphous state in NLCs.

6.4.5 Characterization of optimized Luliconazole and Tavaborole NLCs based gel

6.4.5.1 Viscosity of gel

The viscosity of free Luliconazole gel and LZ NLCs based gel was found to be 1172 ± 0.256 cPs and 1305 ± 0.362 cPs, respectively. The increase in viscosity of NLCs based gel as compared to free Luliconazole gel further leads to higher retention of NLCs based gel on the skin.

The viscosity of free Tavaborole gel and TB NLCs based gel was found to be 1543 ± 0.543 cPs and 1831 ± 0.291 cPs, respectively. The increase in viscosity of NLCs based gel as compared to free Tavaborole gel further leads to higher retention of NLCs based gel on the skin.

6.4.5.2 Spreadability of gel

The spreadability of free Luliconazole gel and LZ NLCs based gel was found to be 11.21 ± 1.54 gm.cm/sec and 18.75 ± 1.75 gm.cm/sec, respectively, demonstrates the good spreadability of the formulated gel. The spreadability of free Tavaborole gel and Tavaborole NLCs based gel was found to be 9.38 ± 1.02 gm.cm/sec and 19.03 ± 1.62 gm.cm/sec, respectively, demonstrates the good spreadability of the formulated gel.

6.4.5.3 pH of gel

The pH of free Luliconazole gel and Luliconazole NLCs based gel was found to be 6.0±0.12 and 6.4±0.31, respectively, clearly resembles the pH of the skin thereby preventing irritation.

The pH of free Tavaborole gel and Tavaborole NLCs based gel was found to be 5.9±0.48 and 6.3±1.28, respectively, clearly resembles the pH of the skin thereby preventing irritation.

6.4.5.4 Assay of gel

The Luliconazole content in free Luliconazole gel and Tavaborole content in Tavaborole free gel was found to be 98.43 ± 1.32 % (9.843 mg/gm) and 98.21 ± 0.18 % (49.11 mg/gm) respectively. Drug content analysis revealed that Luliconazole and Tavaborole were present at 96.88 ± 0.61% (9.69 mg/gm) and 96.49 ± 0.22% (48.25 mg/gm) in their respective nanoemulsion-based gels, indicating a slight decrease from their free gel forms but still within an acceptable range.

6.4.5.5 Gel Strength

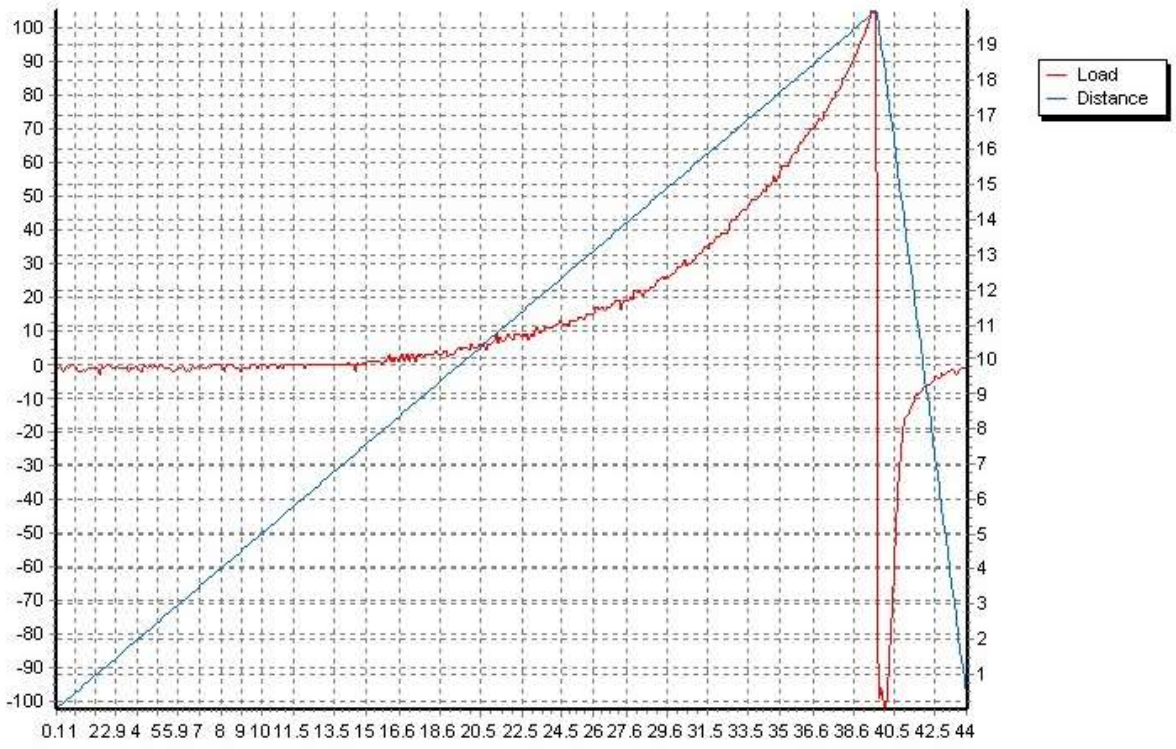

Figure 6.41: Gel strength of Luliconazole loaded NLCs

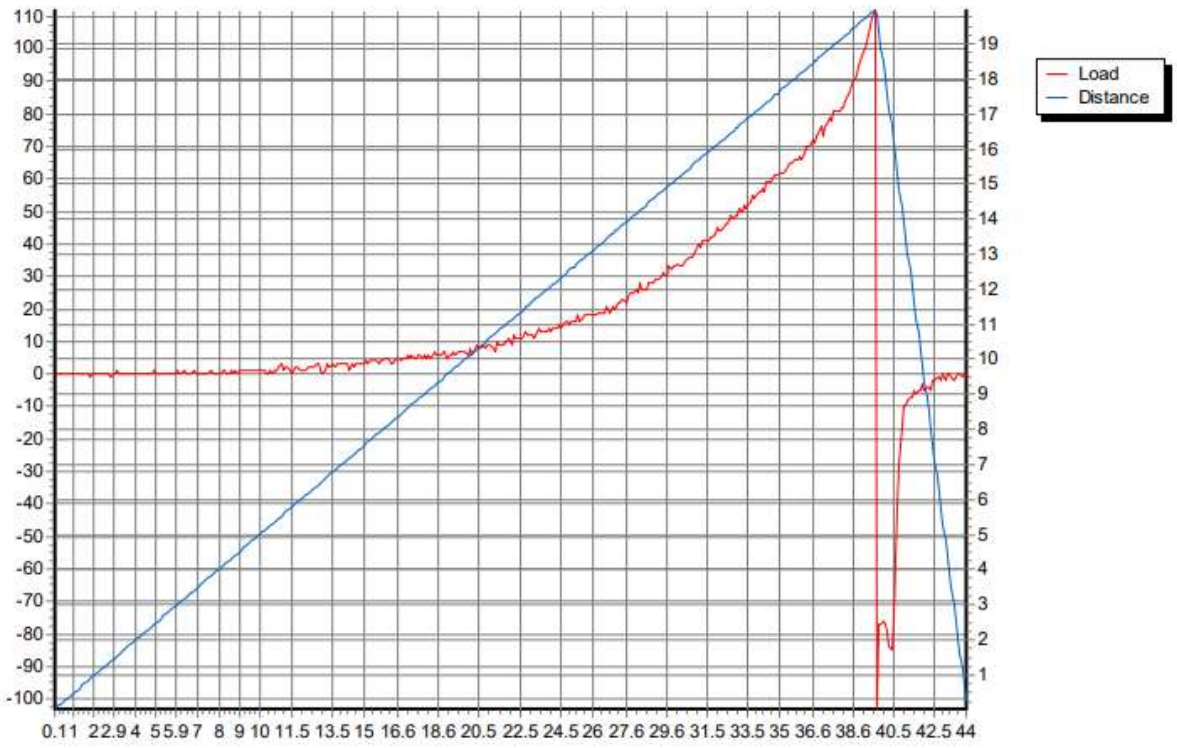

Figure 6.42: Gel strength of Tavaborole loaded NLCs

Gel strength is a measure of a colloidal dispersion's capacity to form and sustain a gel form. Strong gels will withstand far greater pressure than weak gels before being flushed from the site of administration, and it will affect the spreadability and drug's release. This makes gel strength crucial (34). Figure 6.41 and figure 6.42 indicated gel strength of LZ NLCs and TB NLCs 105 gm and 112 gm respectively. Graphs indicate that both gels have significant gel strength.

6.5 References:

1. Gaba, Bharti, et al. "Nanostructured lipid carrier system for topical delivery of terbinafine hydrochloride." *Bulletin of Faculty of Pharmacy, Cairo University* 53.2 (2015): 147-159.
2. Bergsson, Gudmundur, Hilmar Hilmarsson, and Halldor Thormar. "Antibacterial, antiviral and antifungal activities of lipids." *Lipids and essential oils as antimicrobial agents* (2011): 47-80.
3. Müller, Rainer H., Magdalene Radtke, and Sylvia A. Wissing. "Solid lipid nanoparticles (SLN) and nanostructured lipid carriers (NLC) in cosmetic and dermatological preparations." *Advanced drug delivery reviews* 54 (2002): S131-S155.
4. Czajkowska-Kośnik, Anna, Marta Szekalska, and Katarzyna Winnicka. "Nanostructured lipid carriers: A potential use for skin drug delivery systems." *Pharmacological Reports* 71.1 (2019): 156-166.
5. Rocha, Kamilla Amaral David, et al. "Voriconazole-loaded nanostructured lipid carriers (NLC) for drug delivery in deeper regions of the nail plate." *International journal of pharmaceutics* 531.1 (2017): 292-298.
6. Keck, C. M., et al. "A new concept for the treatment of atopic dermatitis: Silver–nanolipid complex (sNLC)." *International journal of pharmaceutics* 462.1-2 (2014): 44-51.
7. Passos, Julia Sapienza, et al. "Development, skin targeting and antifungal efficacy of topical lipid nanoparticles containing itraconazole." *European Journal of Pharmaceutical Sciences* 149 (2020): 105296.
8. Baghel, Saahil, et al. "Luliconazole-loaded nanostructured lipid carriers for topical treatment of superficial Tinea infections." *Dermatologic Therapy* 33.6 (2020): e13959.
9. Salvi, Vedanti R., and Pravin Pawar. "Nanostructured lipid carriers (NLC) system: A novel drug targeting carrier." *Journal of Drug Delivery Science and Technology* 51 (2019): 255-267.
10. Nagaich, Upendra, and Neha Gulati. "Nanostructured lipid carriers (NLC) based controlled release topical gel of clobetasol propionate: design and in vivo characterization." *Drug delivery and translational research* 6 (2016): 289-298.

11. Jahan, Samreen, et al. "Nanostructured lipid carrier for transdermal gliclazide delivery: development and optimization by Box-Behnken design." *Inorganic and Nano-Metal Chemistry* (2022): 1-14.
12. Na, Young-Guk, et al. "Development and evaluation of a film-forming system hybridized with econazole-loaded nanostructured lipid carriers for enhanced antifungal activity against dermatophytes." *Acta biomaterialia* 101 (2020): 507-518.
13. Aslam, Mohammed, et al. "Application of Box–Behnken design for preparation of glibenclamide loaded lipid based nanoparticles: Optimization, in vitro skin permeation, drug release and in vivo pharmacokinetic study." *Journal of Molecular Liquids* 219 (2016): 897-908.
14. Jazuli, Imrana, et al. "Optimization of nanostructured lipid carriers of lurasidone hydrochloride using Box-Behnken design for brain targeting: in vitro and in vivo studies." *Journal of Pharmaceutical Sciences* 108.9 (2019): 3082-3090.
15. Agrawal, Mukta, et al. "Design and optimization of curcumin loaded nano lipid carrier system using Box-Behnken design." *Biomedicine & Pharmacotherapy* 141 (2021): 111919.
16. Haider, Mohamed, et al. "Nanostructured lipid carriers for delivery of chemotherapeutics: A review." *Pharmaceutics* 12.3 (2020): 288.
17. Gordillo-Galeano, Aldemar, and Claudia Elizabeth Mora-Huertas. "Solid lipid nanoparticles and nanostructured lipid carriers: A review emphasizing on particle structure and drug release." *European Journal of Pharmaceutics and Biopharmaceutics* 133 (2018): 285-308.
18. Pardeike, Jana, et al. "Development of an itraconazole-loaded nanostructured lipid carrier (NLC) formulation for pulmonary application." *International journal of pharmaceutics* 419.1-2 (2011): 329-338.
19. Shete, Harshad, and Vandana Patravale. "Long chain lipid based tamoxifen NLC. Part I: Preformulation studies, formulation development and physicochemical characterization." *International journal of pharmaceutics* 454.1 (2013): 573-583.
20. Elmowafy, Mohammed, et al. "Enhancement of bioavailability and pharmacodynamic effects of thymoquinone via nanostructured lipid carrier (NLC) formulation." *Aaps Pharmscitech* 17 (2016): 663-672.

21. Sanad, Rania A., et al. "Formulation of a novel oxybenzone-loaded nanostructured lipid carriers (NLCs)." *Aaps Pharmscitech* 11 (2010): 1684-1694.
22. Nnamani, Petra O., et al. "Development of artemether-loaded nanostructured lipid carrier (NLC) formulation for topical application." *International journal of pharmaceutics* 477.1-2 (2014): 208-217.
23. Kurniawansyah, insan sunan, et al. "Physical characterization of in situ ophthalmic gel: a concise review." *Int J App Pharm* 14.1 (2022): 18-21.
24. Kovačević, Anđelka B., Rainer H. Müller, and Cornelia M. Keck. "Formulation development of lipid nanoparticles: Improved lipid screening and development of tacrolimus loaded nanostructured lipid carriers (NLC)." *International Journal of Pharmaceutics* 576 (2020): 118918.
25. Kovacevic, A., et al. "Polyhydroxy surfactants for the formulation of lipid nanoparticles (SLN and NLC): effects on size, physical stability and particle matrix structure." *International journal of pharmaceutics* 406.1-2 (2011): 163-172.
26. Nagaich, Upendra, and Neha Gulati. "Nanostructured lipid carriers (NLC) based controlled release topical gel of clobetasol propionate: design and in vivo characterization." *Drug delivery and translational research* 6 (2016): 289-298.
27. Yu, Shihui, et al. "Nanostructured lipid carrier (NLC)-based novel hydrogels as potential carriers for nepafenac applied after cataract surgery for the treatment of inflammation: design, characterization and in vitro cellular inhibition and uptake studies." *RSC advances* 7.27 (2017): 16668-16677.
28. Yu, Yibin, et al. "Nanostructured lipid carrier-based pH and temperature dual-responsive hydrogel composed of carboxymethyl chitosan and poloxamer for drug delivery." *International journal of biological macromolecules* 114 (2018): 462-469.
29. Jazuli, Imrana, et al. "Optimization of nanostructured lipid carriers of lurasidone hydrochloride using Box-Behnken design for brain targeting: in vitro and in vivo studies." *Journal of Pharmaceutical Sciences* 108.9 (2019): 3082-3090.
30. Jahan, Samreen, et al. "Nanostructured lipid carrier for transdermal gliclazide delivery: development and optimization by Box-Behnken design." *Inorganic and Nano-Metal Chemistry* (2022): 1-14.

31. Choi, Woo-Sik, et al. "Enhanced occlusiveness of nanostructured lipid carrier (NLC)-based carbogel as a skin moisturizing vehicle." *Journal of Pharmaceutical Investigation* 40.6 (2010): 373-378.
32. Souto, E. B., et al. "Development of a controlled release formulation based on SLN and NLC for topical clotrimazole delivery." *International journal of pharmaceutics* 278.1 (2004): 71-77.
33. Czajkowska-Kośnik, Anna, Emilia Szymańska, and Katarzyna Winnicka. "Nanostructured Lipid Carriers (NLC)-Based Gel Formulations as Etodolac Delivery: From Gel Preparation to Permeation Study." *Molecules* 28.1 (2022): 235.
34. Khurana, S., N. K. Jain, and P. M. S. Bedi. "Development and characterization of a novel controlled release drug delivery system based on nanostructured lipid carriers gel for meloxicam." *Life sciences* 93.21 (2013): 763-772.